Mollusk carbonate thermal behaviour and its implications in understanding prehistoric fire events in shell middens

Stefania Milano[1,2*], Susanne Lindauer[3], Amy L. Prendergast[4], Evan A. Hill[5], Chris O. Hunt[6], Graeme Barker[7], Bernd R. Schöne[2]

[1] Department of Human Evolution, Max Planck Institute for Evolutionary Anthropology, Deutscher Platz 6, 04103 Leipzig, Germany
[2] Institute of Geosciences, University of Mainz, Joh.-J.-Becherweg 21, 55128 Mainz, Germany
[3] Curt-Engelhorn-Zentrum Archaeometry gGmbH, Klaus-Tschira-Archaeometry-Centre, C4, 8, 68159 Mannheim, Germany.
[4] School of Geography, University of Melbourne, 221 Bouverie St, Carlton, 3053, VIC, Australia
[5] School of Natural and Built Environment, Queens University Belfast, Elmwood Ave, Belfast BT9 6AY, UK
[6] School of Natural Sciences and Psychology, Liverpool John Moores University, Byrom Street, Liverpool, United Kingdom
[7] McDonald Institute for Archaeological Research, University of Cambridge, Downing St, Cambridge CB2 3ER, UK

* Corresponding author. Email: stefania_milano@eva.mpg.de

Keywords: Carbonate phase transformation; Haua Fteah; Shell microstructure; Raman spectroscopy; Thermal-induced diagenesis; Pyrotechnology

Abstract

Archaeological shell middens are particularly important for reconstructing prehistoric human subsistence strategies. However, very little is known about shellfish processing, especially when related to the use of fire for dietary and disposal purposes. To shed light on prehistoric food processing techniques, an experimental study was undertaken on modern gastropod shells (*Phorcus lineatus*). The shells were exposed to high temperatures (200-700 °C) to investigate subsequent mineralogy and macro- and microstructural changes. Afterwards, the three-pronged approach was applied to archaeological shells from Haua Fteah cave, Libya (*Phorcus turbinatus*) and from shell midden sites in the United Arab Emirates (*Anadara uropigimelana* and *Terebralia palustris*) to determine exposure temperatures. Results indicated that shells from the Haua Fteah were exposed to high temperatures (600 - 700 °C) during the Mesolithic period (c. 12.7 - 9 ka), whereas specimens from the Neolithic period (c. 8.5 - 5.4 ka) were mainly exposed to lower temperatures (300 - 500 °C). The thermally-induced changes in *A. uropigimelana* and *T. palustris* shells from the South East Arabian archaeological sites were similar to those seen in *Phorcus* spp. suggesting a broad applicability of the experimental results at an interspecific level. Although heat significantly altered the appearance and mineralogy of the shells, $^{14}C_{AMS}$ ages obtained on burnt shells fit within the expected age ranges for their associated archaeological contexts, indicating that robust radiocarbon ages may still be obtained from burnt shells. Our study indicates that the combination of microstructural and mineralogical observations can provide important information to infer shellfish processing strategies in prehistoric cultures and their change through time.

1. Introduction

Shells grow incrementally throughout the lifetime of mollusks and function as protection and support structures. Shells also serve as excellent palaeoenvironmental archives (i.e. Jones, 1983; Schöne et al., 2004; Butler et al., 2013), because they faithfully record the physical and chemical conditions of their ambient environment and temporal changes to these. Such information is stored in the form of geochemical and structural properties (Epstein, 1953; Goodwin et al., 2001; Schöne, 2008). Sclerochronology is the research field that studies the temporal context of shell chemical composition (i.e. stable isotopes and trace elements) and physical accretionary patterns to produce extremely highly resolved palaeoenvironmental reconstructions (Schöne et al., 2005; Miyaji et al., 2007; Milano et al., 2017; Oschmann, 2009). For example, shell oxygen isotope content ($\delta^{18}O_{shell}$) is routinely used as paleothermometer (Schöne et al., 2005; Ferguson et al., 2011; Prendergast et al., 2013; Prendergast and Schöne, 2017).

A rapidly growing interest in the research field of sclerochronology supports the spread of its methodologies and approaches to different disciplines such as archaeology and environmental biomonitoring (Mannino and Thomas, 2002; Andrus, 2011; Steinhardt et al., 2016; Schöne and Krause, 2016). The analysis of mollusk shell material is especially relevant within the framework of prehistoric archaeology. Shellfish have been an important dietary component since the emergence of anatomically modern humans (~ 300 kyr ago; de Lumley, 1966), due to their easy accessibility, reliable availability throughout the year and source of proteins and micronutrients essential for physical development (Erlandson, 2001; Broadhurst et al., 2002; Marean et al., 2007; Fa, 2008).

The application of sclerochronology substantially broadens the potential use of mollusk shells in archaeology. Besides being suitable palaeoenvironmental archives, the shells become a key tool for understanding the response of human behaviour to climatic changes. For instance, $\delta^{18}O_{shell}$ is used to constrain the season of mollusk collection (Mannino et al., 2007; Burchell et al., 2013; Prendergast et al., 2016). In turn, seasonality provides information on the seasonal mobility of hunter-gatherer societies and helps to identify whether sites were permanently or ephemerally occupied (Shackleton, 1973; Mannino and Thomas, 2002; Eerkens et al., 2013). However, the processes related to mollusk preparation, consumption and disposal are still largely unknown (Milano et al., 2016). In some cases, it has been observed a modification of the shell structure by removal of the gastropod apex with stone tool, thorn or canine tip to allow the mollusk to be sucked out (Girod, 2011). As for bivalves, the shells were sometimes scarred or wholesale smashed (Hammond, 2014). Evidence of pyrotechnology associated with mollusk shell middens suggests that a certain degree of heat exposure may have been involved in some cases (Erlandson et al., 1999; Berna and Goldberg, 2008; Taylor et al., 2011). However, few studies have addressed the reconstruction of such processes in the framework of prehistoric marine resource exploitation (Andrus and Crowe, 2002; Aldeias et al., 2016; Milano et al., 2016) and this study will be the first instance where this has been carried out.

The present study builds upon previous work by Milano et al. (2016) who found that significant structural and chemical changes occurred in modern mollusk shells when they were heated at ≥ 300 °C for 20 minutes or more. Here, we investigate the effects of a shorter heat exposure (5 minutes), since shellfish are generally thought to be processed for short periods of time. To achieve this aim, modern *Phorcus lineatus* are used as a calibration tool to understand the response to thermal treatments at the macro-, microstructural and geochemical level. These findings are then applied to archaeological specimens from the Haua Fteah, eastern Libya (*Phorcus turbinatus*) to test whether high temperatures exposure can be detected in archaeological shells of the same genus using the three-pronged approach developed in the experimental phase. Archaeological specimens from the United Arab Emirates (*Anadara uropigimelana* and *Terebralia palustris*) are used to understand the efficacy of this three-pronged approach on a broader scale to other mollusk species. Furthermore, given the importance of shells for radiocarbon dating coastal sites and the abundance of burnt shells in middens (Douka et al., 2014; Lindauer et al., 2016), we present preliminary results on the influence of thermal alterations on shell radiocarbon dating results.

2. Materials and methods

A total of 41 shells were analysed (Table 1). Fifteen live-collected shells of *P. lineatus* were used for the experimental phase. The archaeological material consisted of eighteen specimens of *P. turbinatus* selected from key occupation contexts in the Mesolithic and Neolithic layers from the Haua Fteah cave in Libya, as well as six specimens of *A. uropigimelana* and two specimens of *T. palustris* from shell midden sites near Kalba in the United Arab Emirates (Fig. 1).

2.1 Shell material: *P. lineatus* and *P. turbinatus*

Phorcus spp. are rocky shore gastropods living in the intertidal zone along the Mediterranean (*P. turbinatus:* Menzies et al., 1992; Schembri et al., 2005; Mannino et al. 2008; Prendergast et al., 2013) and Eastern North Atlantic coasts (*P. lineatus:* Kendall, 1987; Donald et al., 2012; Gutiérrez-Zugasti et al., 2015). Both species are sensitive to seasonal environmental changes, specifically water temperature fluctuations. Furthermore, they are extremely abundant in prehistoric sites of this region (Mannino and Thomas, 2001; Colonese et al., 2011; Hunt et al. 2011; Bosch et al., 2015; Gutiérrez-Zugasti et al., 2015). Therefore, many previous studies have used their geochemical data for palaeoenvironmental reconstructions (Mannino et al., 2003; Colonese et al., 2009; Prendergast et al., 2016).

In the present study, *P. lineatus* (previously known as *Osilinus lineatus* and *Monodonta lineata*) was selected as a modern reference and *P. turbinatus* (previously known as *Osilinus turbinatus*, *Monodonta turbinata* and *Trochocochlea turbinata*) for the archaeological case study. Despite being two distinct species, they share similar shell shape, size and the same microstructural organization and mineralogy and they live within the same microenvironments on the Mediterranean and Atlantic coasts. Their shell consists of two aragonitic layers with specific organizations. The outer shell layer (oSL) is arranged in spherulitic prismatic microstructures whereas the inner shell layer (iSL) consists of nacre (Mannino et al., 2008; Milano et al., 2016). The minor phenotypic and taxonomically relevant differences between the two species in shell coloration and aperture size likely do not influence the structural behaviour of the shell in reaction to thermal stress.

2.2 Shell material: *A. uropigimelana* and *T. palustris*

A. uropigimelana and *T. palustris* inhabit tropical mudflats. *A. uropigimelana* is a bivalve of the Arcidae family (ark clams), which is widely distributed in East Africa and the Central Pacific. It lives in shallow waters (1-8 m) in association with seagrass beds and can reach 45 years of age (Tebano and Paulay, 2001; Petchey et al., 2013). *T. palustris*, also known as mud whelk, is one of the largest gastropods of mangrove-dominated habitats in the Pacific Ocean (Plaziat, 1984; Houbrick, 1991; Carlen and Olafsson, 2002). It is typically found in the intertidal zone and its lifespan is currently unknown. Possibly the adult size is reached after about four years, when it moves from offshore environments into the mangrove settings (Nishihira et al., 2002). Both species are very abundant in the prehistoric record in the Arabian Sea region (Biagi et al., 1984; Beech and Kallweit, 2001; Gardner, 2005; Lindauer et al., 2017).

The shell of *A. uropigimelana* is entirely aragonitic and consists of three layers. The oSL is organized in branching crossed-lamellar structures, the middle shell layer (mSL) is formed of linear-crossed lamellae and the iSL is characterized by irregular complex-crossed lamellae. Likewise, the shell of *T. palustris* is aragonite and is organized in simple-crossed lamellar (oSL and iSL) and linear-crossed lamellar microstructures (mSL). The terminology follows the author´s observations and the description from Carter et al. (2012).

2.3 Modern and archaeological settings

Modern specimens of *P.lineatus* were collected from Praia do Tamariz, Portugal (38.7036 °N, -9.4038 °E) on 10 August 2016. The shells were gathered from a rocky portion in the mid-intertidal zone just outside the estuary of the Tajo River on the Atlantic coast (Fig. 1). To minimize the effects of ontogeny on the stable isotope results, shells with similar sizes were selected. Maximum shell height ranged between 12 and 14.3 mm and the maximum shell width ranged between 13.3. and 15.7 mm. This size class represents the average shell size of *P.lineatus* adult population in the region (da Costa, 2015).

Immediately after collection, the specimens were frozen for about one hour and subsequently the soft tissues were removed.

The archaeological remains of *P. turbinatus* were collected from the Haua Fteah cave, Libya (Fig. 1). The Haua Fteah cave was first excavated in 1951-1955 by Charles McBurney, who cut a 14 m-deep stepped trench from the level of the present cave floor, exposing a deep sequence of occupation dating from the last intergacial to the Holocene (McBurney, 1967). New excavations (ERC:TRANSNAP) coordinated by Prof. Graeme Barker between 2008-2015 reopened the McBurney trench and cut an overlapping series of small trenches down its southern face (Barker et al., 2010, 2012; Farr et al., 2013). Eleven of the eighteen specimens used in this study were from Trench U, a small (0.75 m x 1 m) cutting in the upper 2 m of the sediments which exposed occupation levels of Neolithic character and age. The Neolithic phase in the cave has a modelled age of ca. 8.5 - 5.4 cal. BP (Douka et al., 2014). These shells were excavated in 2012 from contexts 742, 743 and 747. These sediments, especially context 747, were associated with evidence of extensive burning in form of frequent charcoal, visibly charred animal bone and shell, and lithic artefacts with thermoclastic fractures. Seven specimens were selected from Trench M, a 2 m x 1 m trench cut down the same side of the McBurney trench at ca. 2-8 m depth. The specimens were excavated in 2009 and 2010 from contexts 10,002, 10,005 and 10,006, which have been dated to the Early Holocene and can be ascribed to the Mesolithic Capsian phase of occupation defined by McBurney (1967). The sediments were similar in character to those of Trench U in terms of their plentiful evidence for firing events.

The archaeological remains of *A. uropigimelana* and *T. palustris* were excavated from open sites on the Gulf of Oman coast in the United Arab Emirates (Fig. 1). Specimen KS Ana1, KSM UBL Ana2, KK1 Ana3 and KK1 Ana4 came from the shell midden KK1 situated near the mangroves at Kalba, along the northern coast of the Gulf of Oman (Lindauer et al., 2016). Specimen KS Ana1 was found on the beach nearby and it yielded a radiocarbon age of 7328-7113 cal. BP. It may have remained in the mangrove sediments or in the sabkha (salt flat) since Neolithic times or perhaps washed out recently from an archaeological midden where it was found on the beach. This would also explain its good preservation. The shell midden KK1 is at the outermost edge of the sabkha of the mangrove at Kalba and contains only material from the Neolithic, in two distinct phases. These are reflected in the shell ^{14}C ages that range from ca. 7146 - 6946 cal. BP at the base to ca. 6600 - 6450 cal. BP at the surface (1σ).

Specimens K4 SL Ana3, K4 SL GA1, K4 BZ GT1 and K4 BZ UGT1 were excavated from site Kalba K4, lying close to the modern town of Kalba north of a mangrove area. This site has evidence of settlement structures that can be ascribed to the Bronze Age and Iron Age. Two distinct layers (MBZ 1 and MBZ 2) situated close to an Iron Age mudbrick wall contain a large amount of shells, both burnt and unburnt, together with charcoal fragments. The lower layer (MBZ1) contained fewer shells than the immediately overlying layer MBZ2. Both layers are around 30 cm thick. Dating measurements show that both layers can be ascribed to the Middle Bronze Age (Lindauer et al., 2017). The shells of the lower MBZ1 have a mean age of ca. 3882 - 3727 cal. BP and the upper MBZ2 shells of ca. 3695 - 3641 cal. BP. The results are in accordance with the archaeological data from previous excavations (Phillips and Mosseri-Marlio, 2002).

2.4 Experimental design

The experiment on modern shells followed a similar protocol to that described by Milano et al. (2016). However, in this case the shells were exposed to different temperatures for 5 min. The choice of this duration was twofold: (1) to identify potential changes in shell behaviour after short (5 min) heat exposure as compared with the medium (20 min) and long (60 min) heat exposures that were tested in the previous study (Milano et al. 2016) and (2) to attempt to reconstruct the temperatures at which archaeological shellfish were processed. Sparse ethnographic observations (e.g. Meehan, 1977, 1982) as well as modern traditions (e.g. Smith, 1978) suggest that the bivalves are processed for only few minutes before consumption.

The shells were heated at 200 °C, 300 °C, 400 °C, 500 °C, 600 °C and 700 °C in a high temperature tube furnace. Specimens were placed in the furnace when the desired temperature was stabilized to ensure the reproducibility of the experiment and to minimize the noise deriving by temperature fluctuations. In order to record potential weight loss, each shell was weighted before and after the roasting experiment to the nearest 1 mg.

2.5 Shell preparation

To study the specimens, modern and archaeological shells were fully embedded in Struers EpoFix resin and air-dried for 24 hours. This strategy prevented the shells from breaking during the following preparation steps. Each resin block was glued to a plexiglass cube and a low-speed precision saw (Buehler Isomet 1000) was used to cut two sections (ca. 2 mm thick) perpendicular to the growth direction. One section of each specimen was glued to a microscope slide with JB KWIK epoxy resin and was later used for geochemical analyses. The other section was used for SEM observations. All shell sections were ground on a Buehler Metaserv 2000 grinder-polisher machine with silicon carbide papers of different grit sizes (P320, P600, P1200, P2500). After each grinding step, the slabs were immersed in de-ionized water and ultrasonically rinsed for 2 minutes. A Buehler VerduTex cloth with a 3 µm diamond suspension was used to polish the sections. The sections used for SEM analysis were etched for 5 s in 1 vol% HCl and bleached for 30 min in 6 vol% NaOCl, to remove the organic sheets masking the microstructures.

2.6 Macro-, microstructural and mineralogical analyses

Modern shells were photographed before and after the thermal treatments allowing a visual comparison at macroscopic scale. To identify thermal changes, the coloration of the shells was identified according to the Pantone colour system. The sections prepared for the SEM were analysed using a Zeiss Axio Imager.A1m stereomicroscope to record potential changes in the appearance of the two shell layers. Prior to the microstructural analysis, the samples were sputter-coated with a 2 nm-thick layer of platinum using a Leica EM ACE200 Vacuum Coater. The surface of the sections was studied with a 3rd generation LOT Quantum Design Phenom Pro desktop SEM with 10 kV accelerating voltage equipped with a backscatter electron detector. Shell mineralogy was investigated in each shell layer by using a Horiba Jobin Yvon LabRam800 spectrometer equipped with an Olympus BX41 optical microscope. The instrument employed a 532.21 nm laser wavelength, a 400 μm confocal hole, a grating with 1800 grooves/mm, an entrance slit width of 100 μm and 50× long-distance objective lens. The integration time of each scan ranged between 3 and 5 s.

2.7 Stable isotope analysis

The stable isotope composition of the modern specimens was analysed on carbonate powder sampled after heating the shells. Carbonate material was obtained from each shell by microdrilling the inner layer (nacre) with a Rexim Minimo dental drill mounted to a stereomicroscope and equipped with a conical drill bit of 300 μm in diameter (Komet/Gebr. Brasseler GmbH & Co. KG, model no. H52 104 003). A Thermo Fisher MAT 253 gas source isotope ratio mass spectrometer in continuous flow mode coupled to a GasBench II at the Institute of Geosciences, University of Mainz was used to analyse the carbonate samples by phosphoric acid digestion (70 °C for 120 min). The isotope data were calibrated against a NBS-19 calibrated Carrara marble standard ($\delta^{18}O$ = - 1.91 ‰). The average internal precision (1σ) was

0.03‰ and the external reproducibility (1σ) was 0.05‰. The $\delta^{18}O$ profiles of the heated shells were compared to the $\delta^{18}O$ profiles of the control specimens, which were not exposed to high-temperature treatments.

2.8 Radiocarbon dating

For radiocarbon dating, small chips were taken near the apex of three *P. turbinatus* specimens. In order to avoid any contamination from sedimentary calcium carbonate or a mixture of different shell layers, the external layer of the shells was physically removed. The fragments of nacre were further processed at the Curt-Engelhorn-Center for Archaeometry, Mannheim, Germany. The material was acidified in phosphoric acid at 70 °C by using an Autosampler system and measured using the MICADAS system (Kromer et al., 2013; Wacker et al., 2013). The results were calibrated with the Marine13 curve (Reimer et al., 2013) and corrected using the Mediterranean reservoir correction (ΔR) of 58 ± 85 ^{14}C years (Reimer and McCormac, 2002) using OxCal v.4.3.2.

2.9 Statistical analyses

ANOVA, Mann-Whitney and Tukey´s HSD post hoc tests were performed using the software PAST to test whether the 5-minute heat exposure had a significant effect on shell geochemistry as well as whether the different durations changed the oxygen isotopic signatures.

3. Results

3.1 Experimental results on the effect of roasting on the shells

At macroscopic level, the 5-minute thermal treatment caused a similar effect as reported for *P. turbinatus* in the previous experiment by Milano et al. (2016), in which shells were roasted for 20 minutes and 60 minutes. Visible alteration of the shell surface occurred at temperatures higher than 200 °C. For instance, the typical background cream coloration (Pantone: 7497 C) alternated with pigmented blotches (438 C) started to change at 300 °C, when the shells acquired a dark coloration with a tendency toward a brown shade (background: 7531 C; blotches: 7518 C). At 400 and 500 °C, the shells became grey (background: 404 C; blotches: 417 C) and the outer shell layer started to detach. At 600 °C, the coloration only slightly changed (background: 416 C; blotches: 417 C) and the material brittleness increased, whereas at 700 °C, the coloration turned into a cream-white tone (background and blotches: 401 C; Fig. 2A). Furthermore, the heat exposure induced a 14 to 25% weight loss, with a greater loss at higher temperatures (Fig. 2B).

At the microstructural level, roasting at 200 °C did not cause any visible change of the shell microstructure. First-order and second-order prisms (oSL) and platelets (iSL) of the heated samples did not appreciably differ from those of unheated samples. At 300 °C, the oSL did not show any visible alteration whereas the nacre platelets became slightly porous with nanometer sized holes appearing on their surfaces (Fig. 2C-D). At 400 °C, the single second-order prisms of the oSL were still recognizable. However, sheets of organic material emerged between the first-order prisms partially covering the shell surface. The platelets of the nacre started to fuse and large cracks developed on the surface. After heating at 500 °C, the oSL underwent a significant transformation with the formation of new irregular-shaped units surrounded by organic sheets. Meanwhile, the iSL surface was partially covered by organic matter which emerged from the inter-lamellar voids that formed at 400 °C (Fig. 2C-D). The appearance of the oSL at 600 °C is very similar to the previous treatment (500 °C) with an enhanced presence of organic material. The platelets of the nacre showed a higher degree of fusion in every direction with large quantities of organics in between them. At 700 °C, the surface of the biomineral units of the oSL units became more compact with a decrease in porosity. At the same time, the agglomeration of the iSL platelets led to the formation of new boundaries delineating larger and irregular units (Fig. 2C-D).

The shell mineralogy was also affected by heat (Fig. 2C-D). Originally, the shells were fully aragonitic as indicated by Raman peaks at 152 cm^{-1},180 cm^{-1}, 207 cm^{-1},707 $cm^{-1}$and 1086 cm^{-1}. The transition from aragonite into calcite started at 400 °C in the oSL and is indicated by an extra peak at 281 cm^{-1} (Fig. 2C). At this temperature, however, the iSL was still completely aragonitic. At 500 °C, both layers were transformed into calcite with peaks at 153 cm^{-1}, 281 cm^{-1}, 713 cm^{-1} and 1086 cm^{-1}.

Similar to our previous results (Milano et al. 2016), the shell oxygen isotope composition changed in response to the heat treatment. The $\delta^{18}O_{shell}$ values of the control sample ranged between - 1.0 and + 1.0 ‰. The oxygen isotope range is more negative than the range obtained by the control shells used in Milano et al. (2016). This offset reflects the difference of the local environments. The shells from Portugal used in the present study were collected from an area characterized by much larger freshwater input, and hence lower $\delta^{18}O_{shell}$ values, than the specimens from Libya used in Milano et al. (2016). The oxygen isotope composition of shells processed at 200 °C and 300 °C for 5 mins ranged between - 0.5 and + 0.7 ‰ (Fig. 3A). According to the Mann-Whitney *u*-test there is no statistical difference between these heated samples and the control shells ($p > 0.05$; Fig. 3B). The effect of the shell exposure at 400 °C could not be tested, because the nacre layer was too thin to obtain sufficient carbonate powder. As expected, higher temperatures (500 - 700 °C) had a significant influence on $\delta^{18}O_{shell.}$ Average values were offset by -1.5 ‰ ± 0.2 with respect to the average values of the control material. Minimum and maximum values were offset by -0.8 ‰ ± 0.1 and -0.8 ‰ ± 0.7, respectively (Fig. 3A). The oxygen isotopic composition of the shells heated over 500 °C was statistically different from the lower temperature treatments and the control conditions (Mann-Whitney test $p < 0.05$; Fig. 3B). A comparison between the current data and the results published in Milano et al. (2016) was used to determine the influence of the duration of the heating process on the shell. The offsets of the $\delta^{18}O_{shell}$ values from the respective control values were calculated for the three duration treatments (5, 20 and 60 min). The offsets of minimum, average and maximum $\delta^{18}O_{shell}$ values were statistically similar among all treatment durations (ANOVA $p > 0.05$).

3.3 Archaeological shells: structural and mineralogical organization

The *P. turbinatus* specimens from the Haua Fteah presented inter-individual differences in their appearance at macroscopic scale (Fig. 4). All of the Mesolithic specimens (Trench M) showed a homogenous dark grey surface with areas of partial detachment of the oSL (i.e. M002_1 in Fig. 4D, Supplementary material Fig. S1). The nacre was less uniform and lighter grey in colour. In general, these shells looked similar to those of the experiment roasted at 600 °C (Fig. 2A). Two specimens from the Neolithic context 747 (U747_1 and U747_2) were lighter grey and looked similar to shells heated at 500 °C (Supplementary material Fig. S1). The third specimen from this layer (U747_3) showed an iridescent iSL and an overall coloration likely related to lower heating temperatures (i.e., 300 °C; Supplementary material Fig. S1). All four Neolithic *P. turbinatus* specimens from context 743 were light brown in colour and showed iridescent nacre (i.e. U743_3 in Fig. 4B). The same applied to the two shells from context 742 (U742_2 and U742_4; Fig. 4A, Supplementary material Fig. S1), whereas U742_1 and U742_3 were grey as if subjected to higher temperatures (Fig. 4C, Supplementary material Fig. S1).

In good agreement with the observations of the macro appearance of the shells, microstructures varied greatly between individuals. The prisms in the oSLs of the Mesolithic specimens from were replaced by porous irregular units and the nacre platelets were fused together into larger agglomerates (Fig. 4D, Supplementary material Fig. S2). The integral microstructural reorganization and the subsequent absence of any of original secondary prisms (oSL) and platelets (iSL) recall the structural arrangement of the modern samples exposed to high temperatures (600 °C; Tab. 2). A similar architecture was observed in the Neolithic specimens U747_1, U747_2 and U742_3. On the other hand, all shells from context 743 and specimens U747_3 and U742_4 showed well-defined prismatic structures in the oSL and slightly porous platelets in the iSL, which looked similar to the experimental shells heated at 300 °C (Fig. 4B, Supplementary material Fig. S2). Shell U742_1 represented the only case identifiable as processed at a temperature of ca. 500 °C (Table 2). The prisms of the oSL appeared to have undergone major fusion at 400 °C (Fig. 4C). However, the single elongated prisms were still partially visible and they were not completely transformed as in the case of the material burned at 600 °C. A similar pattern was observed in the nacre, where the agglomerations of platelets started to define new structural units (Fig. 4C). The microstructures of specimen U742_2 were perfectly preserved and did not show any sign of thermal alteration (Fig. 4A, Table 2).

According to Raman spectroscopy, seven shells were entirely aragonitic and eleven were calcitic (Fig. 5). All Mesolithic specimens and four of the Neolithic specimens consisted of calcite (Fig. 5A), whereas the remaining specimens from Trench U were aragonitic (Fig. 5B). No transition phase was detected and the two shell layers always shared the same mineralogy. Based on the results presented above, the calcitic shells were categorized as having been exposed to temperatures in excess of 500 °C (Tab. 2).

Similar to the *P. turbinatus*, some archaeological specimens of *A. uropigimelana* and *T. palustris* from the United Arab Emirates sites displayed an altered overall appearance (Fig. 6). Shells K4 SL Ana3, KSM UBL Ana2, KK1 Ana3 and KK1 Ana4 showed the characteristic homogenous creamy colour of unaltered *A. uropigimelana* (Fig. 6A; Supplementary material Fig. S3). A slightly darker shade, especially on the inner shell surface, was visible in KK1 Ana4. Two shells, KS Ana1 and K4 SL GA1, showed a grey shell surface. The first was characterized by a light tone, whereas the latter was darker with shaded areas on the inner shell surface clearly indicating heat exposure (Fig. 6A; Supplementary material Fig. S3). In the case of *T. palustris*, one specimen (K4 BZ UGT 1) had its surface coloration preserved, whereas a second specimen (K4 BZ GT 1) was very dark (Fig. 6B).

The well-preserved *A. uropigimelana* specimens K4 SL Ana3, KSM UBL Ana2, KS Ana1, KK1 Ana3 and KK1 Ana4 showed well-defined crossed-lamellar structures in the oSL, linear-crossed lamellae in the mSL and irregular complex-crossed lamellae in the iSL. The excellent preservation state was also corroborated by the presence of organic microtubules across the shell layers (Fig. 6A; Supplementary material Fig. S3). Conversely, shell K4 SL GA1 displayed altered microstructures. The first order lamellae of the oSL and mSL were still visible, whereas the morphometric characteristics of the third order lamellae were changed. The units were fused together in large agglomerates with new boundaries (Fig. 6A). These features recall the oSL of *Phorcus* spp. heated at 600 °C. In the iSL, the lamellae lost their individuality and elongated shape, forming compact clusters of material separated by organic sheets and cracks (Fig. 6A). The *T. palustris* specimen K4 BZ UGT 1 showed the typical simple and linear-crossed lamellar microstructures (Fig. 6B), whereas in specimen K4 BZ GT 1 lamellar biomineral units were transformed into large irregular-shaped assemblages in the oSL and iSL. In the mSL, small granular carbonate units with well-defined boundaries prevailed (Fig. 6B). Such alteration was likely related to high temperatures (≥ 500 °C). However, in this case an accurate estimate of the processing temperature cannot be provided based on the microstructures, because no such architecture was previously observed in the mSL.

Typical aragonite Raman spectra occurred in all but two *A. uropigimelana* and *T. palustris* specimens. The mineralogy of K4 SL GA1 and K4 BZ GT 1 was entirely calcitic (Fig. 7A-B).

3.4 Radiocarbon dating of *P. turbinatus* from Haua Fteah

Specimen U742_2, with no sign of heat exposure (Fig. 4A), was dated to 7184 ± 21 ^{14}C yr BP calibrated to 7772 - 7438 cal. BP (2σ). Specimen U742_1, with signs of high temperature exposure (Fig. 4C), was dated to 7300 ± 21 ^{14}C yr BP calibrated to 7901 - 7556 cal. BP. both these dates fit with existing ^{14}C dates for context U742. Specimen U742_3 (Fig. 4B), with burning marks, was dated to 6378 ± 21 ^{14}C yr BP calibrated to 7002 - 6558 cal. BP. These dates fit with the current chronostratraphic understanding of Context U743, which is paired with U742 stratigraphically (Fig. 8). Associated ^{14}C radiocarbon ages are available from other materials dated in Trench U are also included in this study for comparative purposes (Table 3). The relatively broad spread of dates from U742 fits sedimentological model for this part of the Haua Fteah deposition sequence and all sit within the existing age range for these context.

Context U742 is one of a group of chronologically identical contexts (with U743, U744, U746 and U747) that form a cross section of a debris flow that contains archaeological material that can be attributed to the Neolithic.

4. Discussion

4.1 A comparative approach to thermal-induced diagenesis in biogenic carbonates

Diagenesis encompasses all physical and chemical processes occurring to the tissues after the death of the animal. The present study focuses exclusively on thermally-induced diagenesis associated with heat exposure. High temperatures accelerate a process that naturally would require thousands of years. When dealing with archaeological remains it is important to differentiate between the two types of diagenetic processes to ensure a correct interpretation of the results. In order to do so, the whole shell assemblage needs to be taken into consideration. Specimens from a certain archaeological layer are subjected to similar environmental conditions after burial (i.e. depth, sediment composition and soil pH). Therefore they are likely to share similar preservation conditions. The overall preservation state indicates whether natural diagenesis altered the shells or not. Any deviation from the average preservation state is likely related to different processes. In our case, shells without evidence of burning are generally well-preserved suggesting that natural diagenesis did not occur (Prendergast et al., 2016). Any altered shell is likely to be related to heat-induced diagenesis. Although this approach allows a reasonable distinction between natural and artificial diagenesis, further studies on naturally-altered shell material are needed to characterize the structural and mineralogical key features relative to this type of diagenesis.

As previously demonstrated by Milano et al. (2016), the macroscopic and microscopic appearance of *Phorcus* spp. shells gradually altered as the processing temperatures increased. Although the thermal exposure time was reduced to 5 minutes in the present study, similar mineralogical and geochemical changes were observed. The only exception is the temperature at which the aragonite-to-calcite transformation of the oSL occurred, i.e., 400 °C in the present study and 300 °C in Milano et al. (2016). Based on this discrepancy, we suggest that the duration of the thermal exposure may play a role in the development rate of such taphonomic processes. However, time is only of secondary importance in comparison to the actual processing temperature. In good agreement with the most of our results, Aldeais et al. (2016) demonstrated that the mineralogy of *Cerastoderma edule* and *Scrobicularia plana* shells showed no differences after roasting for 5 and 20 minutes. In abiogenic and biogenic minerals, the aragonite-to-calcite and microstructural transformations have been previously observed to occur very rapidly at critical temperatures around 400 °C and 500°C, respectively (Lécuyer, 1996; Koga et al., 2013). As a consequence, it will most likely be impossible to reconstruct the processing duration based on the analysis of archaeological shells, but it is possible to reconstruct the temperatures at which they were exposed. Consequently, it may be possible to postulate the type of fire or fuel that created those temperatures.

P. lineatus shells lost weight after roasting, especially at temperatures above 300 °C (21.5 % weight loss). Heat-induced weight losses have previously been reported from biogenic and abiogenic minerals (Yoshioka and Kitano, 1985; Balmain et al., 1999; Bourrat et al., 2007). Thermal exposure induces a three-step release of water and organic content. At first, the endothermic reaction provokes dehydration through evaporation of the water incorporated in the mineral phase (Yoshioka and Kitano, 1985; Perić et al., 1996; Huang et al., 2009). Then, at temperatures between 250 °C and 450 °C, the organic matter in the shell starts to degrade (Bourrat et al., 2007; Huang et al., 2009). In *Phorcus* spp., this temperature range conforms to the appearance of large organic sheets partially masking the carbonate microstructures (Fig. 2). The degradation intensifies at higher temperatures (> 500 °C) and is associated with weight losses up to 50 % (Balmain et al., 1999; Zolotoyabko and Pokroy, 2007; Huang et al., 2009; Villagran et al., 2011).

In the present study, temperature was increased stepwise by 100 °C steps to systematically investigate structural and mineralogical changes of the shells. The outer shell layer of *P. lineatus* started to transform from aragonite to calcite at 400 °C. This process was completed at 500 °C. In the case of the nacre, no such broad transition phase was detected. Conversion to calcite took place at 500 °C, at which point the iSL was entirely calcitic. According to previous studies, however, polymorphic transition of mollusk shells already started at temperatures of 250 - 350 °C, and conversion to calcite was completed between 400 °C and 500 °C (Lécuyer, 1996; Maritan et al., 2007; Aldeias et al., 2016). Conversion temperatures seem to vary between species. As shown by Aldeias et al. (2016), the mineralogy of *C. edule* and *S. plana* reacts differently to heating. In *C. edule* polymorphic conversion occurs between 250 and 500 °C, whereas in *S. plana* the transformation only starts at 350 °C and is completed at 400 °C. The observed differences in polymorphic conversion temperatures may be explained by specific structural properties of the materials. Crystal morphology and crystallography were previously identified as potential factors controlling mineralogical transformations (Koga et al., 2013). In abiotic systems, aragonite crystals split and released water trapped within them. Furthermore, calcite nucleation occurs preferably along mineral cracks and twin boundaries (Bischoff and Fyfe, 1968; Liu and Yund, 1993). For these reasons, crystal characteristics and positions of boundaries influence the conversion reaction (Koga et al., 2013). The architectural diversity among mollusk species and shell layers may be the origin of the variable reaction of different biominerals to thermal stress (Kobayashi and Samata, 2006). Aragonitic mineral units tend to lose density and acquire nanopores on their surfaces, while a network of cracks forms in the material (Perdikouri et al., 2011; Villagran et al., 2011; Gomez-Villalba et al., 2012). These features were also observed in the present study in *P. lineatus* specimens roasted at 400 °C, i.e., before full conversion into calcite.

Given the complexity in the thermal behaviour of biogenic materials, the three-pronged approach of mineralogical, macro- and microscopic observations is essential to better understand the thermally-induced diagenetic processes. The identification of specific changes in the shell can be used as indicator of shell processing temperatures, although possibly with some differences from species to species.

4.2 Implications of heat exposure for palaeoenvironmental reconstructions

Heat exposure can induce an exchange of oxygen isotopes with the surrounding environment, drastically altering initial shell isotopic composition (Andrus and Crowe, 2002; Milano et al., 2016). Temperatures higher than 300 °C are observed to cause a significant decrease in $\delta^{18}O_{shell}$ (Milano et al., 2016). Our results are in good agreement with the previous findings suggesting that the use of burnt mollusk shells may have important implications for palaeoenvironmental reconstructions. A decrease in $\delta^{18}O_{shell}$ translates into an overestimation of the reconstructed water temperature, which can jeopardize the reliability of related reconstructions. Furthermore, burning at high temperatures can influence the results of palaeoseasonality studies by incorrectly estimating the season(s) of mollusk collection, which in turn may affect the interpretation of hunter-gatherer mobility and settlement use.

It is recommended to discard shells with signs of thermal exposure for isotopic analyses. However, it has to be noted that not all heating intensities imply isotopic alteration. Low temperatures (< 300 °C) do not induce significant changes in the $\delta^{18}O_{shell}$. Shells exposed to such temperatures can still be used to accurately estimate palaeotemperatures. However, a careful analysis is needed to differentiate between the different heat exposures and to ensure an optimal sample selection for isotopic studies. It is also advisable to avoid any form of pre-treatment involving heating, which was commonly adopted in the past as method for organic matter removal (Mook, 1971).

4.3 Prehistoric fire events and shell middens

Different types of fire events can be associated to shell middens, according to their nature and use. The first evidence for controlled fire is dated to around 300,000-250,000 years ago and it is related to a change in hominin habits, especially concerning diet (James et al., 1989; Shahack-Gross et al., 2014; Gowlett, 2016). Among the main benefits of using fire for dietary purposes are the maximization of energy gain and food digestibility and the development of social abilities such as storing, sharing and processing food (Ragir, 2000; Wrangham and Conklin-Brittain, 2003; Wrangham, 2009; Wrangham and Carmody, 2010). Several ethnographic studies suggest that cooking may play an important role in shellfish consumption (Percy, 1608; Meehan, 1977, 1982). Cooking is generally known to facilitate the extraction of the edible portion. In fact, the heat weakens the muscle attachment of the mollusks causing the valves to open (bivalves) and the flesh to detach more easily. In Australia and North America mollusks were placed over or underneath fire, coals or hot stones (Kroeber and Barrett, 1960; Beaglehole, 1974; Bailey, 1977). In other cases, they were cooked in earth ovens (Meehan, 1982; Waselkov, 1987; Thoms, 2008). Additionally, steaming was adopted as an alternative technique by some ethnic groups such as the Maori in New Zealand and the Quileute and the Tlingit in the Pacific Northwest (Best, 1924; Reagan, 1934; Newton and Moss, 1984). Generally, the cooking processes were rather fast, possibly lasting only a few minutes (Meehan, 1977; Thoms, 2008). After being cooked, mollusk soft tissues were sometimes dried or smoked to enable storage for longer periods of time and for trading purposes (Greengo, 1952; Moss, 1993). In addition to food preparation, fire could have being used for trash disposal (Ford, 1989). Ethnographic observations by Meehan (1982) describe occasional burning of food debris by igniting grass on top of large mounds of disposed shells. However, in other cases, the shells were arranged in heaps and covered with sand, without involving any fire (Bird and Bird, 1997). Alternatively, Mougne et al. (2014) suggested the shell refuses to be directly thrown into a fire.

To contextualize our results in the light of the ethnographic records, the experimental work by Aldeias et al. (2016) simulating different firing techniques offers a valuable source of information. The authors showed that when a fire was set on top or underneath a pile of shells, there was a great degree of heterogeneity in the shell mineralogical response. The heat diffusion affected differently the single specimens according to their position in respect to the heat source, resulting in a mixture of aragonitic and calcitic shells. Our results indicate that the distribution of specific burning-related features is generally shared among the specimens of the same layer suggesting a homogenous exposure to heat. An exception to this trend is represented by the shells from the Neolithic layer U742, which will be discussed further below. Such uniform heat exposure likely implies heating of relatively small quantities of shells with a similar position in respect to the fire whereas large amounts of material, characteristic of disposal mounds, would induce a significant spatial heat gradient and diverse thermal response. Furthermore, concerning the food disposal by throwing the shells into the fire, this involves direct contact with extreme temperatures. Under these circumstances, the shells would become extremely brittle and prone to a rapid disintegration with limited chances of fossil 'survival' (Milano et al., 2016). In this perspective, our data conform better with firing events associated to food processing rather than food disposal. However, further analysis on additional material is needed before unequivocally discriminate between the two different types of fire.

Estimation of shellfish heating temperatures from the Haua Fteah suggests a clear distinction between the two archaeological contexts studied here. The seven Mesolithic shells all appear to have been exposed to temperatures between 600 and 700 °C. These temperatures can be reached when the shellfish are situated in close proximity to the heat source without being directly in contact with it. Temperatures between 633 and 781 °C were recorded when experimentally roasting the mollusks on a surface with fuel and fire on top of them (Aldeias et al., 2016). Such temperatures fit well with our observations on the shell remains. However, it has to be considered that roasting temperatures also largely depend on the type of fuel used. In the experiments by Aldeias et al. (2016), pine wood and pine needles were adopted, whereas grass material is known to burn at lower temperatures (max. 430 °C; Wolf et al., 2013). In the light of these observations and our own results, shellfish during the Mesolithic phase at the Haua Fteah were probably processed underneath woody fires.

In contrast, the Neolithic shells from the Haua Fteah layers U747 and U743 have features pointing to lower temperature exposure: ca 71 % were heated at temperatures around 300 °C. The drastic increase in remains exposed to lower temperatures in the Neolithic phase can be explained by changes in the shellfish processing. A potential interpretation is related to the appearance of the first pottery during the Neolithic, which could have been used to prepare shellfish (McBurney, 1967; Douka et al., 2014; Prendergast et al., 2016). Although the use of vessels for processing marine resources has not been yet attested around the Mediterranean during the Neolithic (Debono Spiteri and Craig, 2014), it has been previously observed in other regions (Craig et al., 2011; Taché and Craig, 2015). An experiment conducted by Maggetti et al. (2011) showed that clay pots exposed to fire can reach temperatures of around 300 °C after ca. 10 minutes, supporting our observations in the shells of layers U747 and U743. A second interpretation of the lower temperature exposure during the Neolithic encompasses similar heating processes with the adoption of substantially different types of fuel. As mentioned above, the usage of grasses as fuel could explain the lower burning temperatures experienced by the Neolithic shells.

As an exception to the general trend observed in the results, the shells from unit U742 present heterogeneous burning features related to temperatures from 300 °C to 600 °C, with one shell without any burning sign. On the basis of our observations two hypotheses can be discussed. Different burning degrees may indicate the presence of a thermal gradient related with the use of fire for disposal purposes. Alternatively, the shell may reveal changes in cooking processes in relation to the type of fuel used and/or cooking vessels adoption.

In the case of the archaeological samples from the United Arab Emirates, both species showed evidences related to heating at 500 - 600 °C. Archaeological sites in this area dated to the late Bronze Age or Classic Wadi Suq period (2000 - 1500 BC) are characterized by a large amount of pottery remains such as beakers and spouted globular jars (Carter, 1997). In this region, food processing with pots seems to have appeared during the Bronze Age, whereas roasting on fire was the preferred method in earlier times (Händel, 2013). However, the small sample size considered in the present study does not allow us a more precise interpretation. In order to better understand the evolution of shellfish processing in the area, additional specimens are needed.

Together with intentional fires, natural burning events can occur in shell middens. A distinction between intentional and unintentional firing events can hardly be determined on the basis of shell thermal response. However, as in the case of disposal by directly throwing the shells into fire, long-lasting uncontrolled fires would lead to the complete disappearance of the shell remains within the midden. In our case, the preservation of large fragments and whole shells suggests that the heat exposure was likely not related to long-lasting natural fires. However, rapid fires cannot fully be discharge as potential burning sources.

4.4 Heat exposure and radiocarbon dating robustness

Previous studies on shell-tempered pottery showed that these materials provide consistent $^{14}C_{AMS}$ dates (Rick and Lowery, 2013). To obtain resistant ceramics, shell-tempered pottery is typically fired at 300 - 600 °C and - after cooling - fired again to 500 - 600 °C (Kingery et al., 1976; Herbert, 2008). Such temperatures do not seem to affect radiocarbon ages on the shell inclusions, which fit well with dates from charcoal and bone fragments of the same context (Rick and Lowery, 2013). Shells analysed in the present study did not differ from already available ages of the same stratigraphic context. According to the structural and mineralogical analyses, two of the samples were burned at 500 °C and 600 °C, whereas the third one was not burned. The relatively homogeneous AMS dates suggest that heating does not affect radiocarbon ages, even when polymorphic transformation has occurred. This may be due to the fact that the extremely small quantity of carbon remaining in the material (ca 0.1 wt%) is still enough to allow AMS dating (Lanting et al., 2001). Furthermore, physical alterations of the biomineral such as structural unit enlargement and recrystallization seem to provide a barrier protecting the remaining carbon (van Strydonck et al., 2005).

4.5 Methods to identify thermal exposure on shell remains

Our results show that the overall appearance of shells alone is an insufficient approach to identify heating-related changes (Milano et al., 2016). Although useful in cases of exposure to high temperatures with evident burning marks, examination by the naked eye has important limitations when it comes to lower temperatures. For instance, based on the outer shell layer, specimen U742_2 seemed to have been exposed to 300 °C. However, according to more detailed analysis using SEM it turned out to be untreated.

The analysis of the mineralogical response to heat is valuable when combined with other methods. However, it may prove ambiguous when used alone. The archaeological material analyzed for this study did not show any carbonate polymorph transition phase. Therefore, Raman spectroscopy could only help to distinguish between temperatures below and above 500 °C. Our current and previous results indicate that a combined approach of optical microscopy, SEM and Raman spectroscopy is the most suitable solution to identify alterations related to shellfish processing. The combined use to these techniques will provide more robust data on heating exposure, whether the aim of the research is to preclude heated shells for palaeotemperature reconstructions (Milano et al., 2016) or to examine the food processing in more detail. Although the experimental phase was specifically designed for *Phorcus* spp., the observations showed similarities with the thermal behaviour of *A. uropigimelana* and *T. palustris*. Such analogy in the responses to heat suggests that temperature estimation can be achieved among different mollusk species even without a specific foregoing experimental phase. Results of our findings can be used to answer a broad spectrum of different questions in the framework of shell midden research and shell-tempered pottery studies. Further studies on calcite mollusk shells are needed to complement the existing data on aragonite shells. This will improve the understanding of the biomineralized tissue thermal response in the case of a more stable calcium carbonate phase.

Although the methodology developed offers a powerful toolbox to reconstruct shell thermal exposure, care must be paid when interpreting the results in the archaeological context. As discussed, the preservation conditions of the shells (i.e., entire shells/small fragments; homogenous/heterogeneous burning features) can offer insights into the type of fire event. However, these parameters cannot resolve with certainty the exact nature of the fire (intentional/natural; cooking-related/disposal-related). Furthermore, it is important to mention that, given the irreversible nature of the structural and mineralogical thermal response, multiple burning events cannot be discerned. As for any study on burnt remains, the signature preserved is related to the highest temperature experienced by the shell material.

5. Conclusions

The experimental component of this study has confirmed that shellfish processing methods encompassing temperatures greater than or equal to 300 °C do significantly alter mollusk shell material, but that the duration of the heating does not appear to significantly affect the behaviour of the shell to thermal treatment. According to these findings, structural and chemical changes occur as soon as the shell is exposed to high temperatures. The results also confirm that using burnt shells for palaeoenvironmental reconstructions can produce incorrect temperature estimations and affect the interpretation of environmental and human-related conditions. One proviso to these findings is that the experiments were conducted on fresh shell from which the flesh had been removed when the live mollusks were collected, and further experimental work is needed to establish what impact the presence of body fluids might have on the results. However, burned shells remain a valuable source of information. The experimental changes observed in the modern shells at macro-, microstructural and mineralogical scales have allowed us to determine a set of criteria to detect heating temperatures that can easily be applied to archaeological shells. Analysis of archaeological shells of *P. turbinatus* from the Haua Fteah cave in coastal northeast Libya revealed that during the Mesolithic the shells were uniformly exposed to high temperatures (shells in close proximity to the heat source) whereas during the Neolithic lower temperatures were recorded. Although, the use of fire for non-dietary purposes cannot be completely ruled out, the trend in our results can be interpreted as a temporal change in shellfish preparation.

Analysis of archaeological shells of *A. uropigimelana* and *T.palustris* from Neolithic and Bronze Age shell midden sites on the coast of the United Arab Emirates found that some specimens did not show any evidence of burning while others showed indications of high-temperature exposure. Although burning affected the shell structure and mineralogy, it does not appear to have a significant influence on radiocarbon ages suggesting the possibility of using burnt remains for dating purposes. The fact that the thermal reaction of different species is similar provides confidence in applying the techniques outlined in this study at an interspecific level.

Acknowledgements

The authors thank Michael Maus and Dr. Tobias Häger for helping during isotope analysis and Raman measurements and Dr. Lucy Farr for selecting the shells from the Haua Fteah assemblage. Funding for this study was kindly provided by the EU within the framework (FP7) of the Marie Curie International Training Network ARAMACC (604802) to SM and by the Alexander von Humboldt Postdoctoral Fellowship (1151310) and McKenzie Postdoctoral Fellowship to AP. The Haua Fteah excavations were undertaken with the permission of the Libyan Department of Antiquities and with funding to GB from the Society for Libyan Studies and from the European Research Council (Advanced Investigator Grant 230421), whose support is also gratefully acknowledged. The three anonymous reviewers are thanked for their constructive comments on the manuscript.

References

Aldeias, V., Gur-Arieh, S., Maria, R., Monteiro, P., Cura, P., 2016. Shell we cook it? An experimental approach to the microarchaeological record of shellfish roasting. Archaeol. Anthropol. Sci. doi:10.1007/s12520-016-0413-1

Andrus, C.F.T., 2011. Shell midden sclerochronology. Quat. Sci. Rev. 30, 2892-2905. doi:10.1016/j.quascirev.2011.07.016

Andrus, C.F.T., Crowe, D.E., 2002. Alteration of otolith aragonite: Effects of prehistoric cooking methods on otolith chemistry. J. Archaeol. Sci. 29, 291-299. doi:10.1006/jasc.2001.0694

Bailey, G.N., 1977. Shell mounds, shell middens, and raised beaches in the Cape York Peninsula. Mankind 11, 132-143.

Balmain, J., Hannoyer, B., Lopez, E., 1999. Fourier transform infrared spectroscopy (FTIR) and XRD analyses of mineral and organic matrix during heating of mother of pearl (nacre) from the shell of the mollusc *Pinctada maxima*. J. Biomed. Mater. Res. 48, 749-754. doi:10.1002/(SICI)1097-4636(1999)48

Barker, G., Bennett, P., Farr, L., Hill, E., Hunt, C., Lucarini, G., Morales, J., Mutri, G., Prendergast, A.L., Pryor, A., Rabett, R., Reynolds, T., Spry-Marques, P., Twati, M., 2012. The Cyrenaican Prehistory Project 2012: the fifth season of investigations of the Haua Fteah cave. Libyan Stud. 43, 115-136. doi:10.1017/S026371890000008X

Beaglehole, J.C., 1974 (ed.), The Journals of Captain James Cook on his Voyages of Discovery: The Voyage of the Endeavor, 1768-1771. Hakluyt Society, Cambridge.

Beech, M., Kallweit, H., 2001. A note on the archaeological and environmental remains from site JH57, a 5th-4th millennium BC shell midden in Jazirat al-Hamra, Ra´s al-Khaimah. Tribulus 11, 17-20.

Berna, F., Goldberg, P., 2008. Assessing Paleolithic pyrotechnology and associated hominin behaviour in Israel. Isr. J. Earth Sci. 56, 107-121. doi:10.1560/IJES.56.2-4.107

Best, E., 1924. The Maori. Volume 2. Wellington

Biagi, P., Torke, W., Tosi, M., Uerpmann, H., 1984. Qurum : a case study of coastal archaeology in Northern Oman. Coast. Archaeol. 16, 43-61.

Bird, D.W., Bliege Bird, R.L., 1997. Contemporary shellfish gathering strategies among the Meriam of the Torres Strait Islands, Australia: Testing predictions of a central place foraging model. J. Archaeol. Sci. 24, 39–63. https://doi.org/10.1006/jasc.1995.0095

Bischoff, J.L., Fyfe, W.S., 1968. Catalysis, inhibition, and the calcite-aragonite problem: I. The calcite-aragonite transformation. Am. J. Sci. doi:10.2475/ajs.266.2.80

Bosch, M.D., Wesselingh, F.P., Mannino, M.A., 2015. The Ksâr 'Akil (Lebanon) mollusc assemblage: Zooarchaeological and taphonomic investigations. Quat. Int. 390, 85-101. doi:10.1016/j.quaint.2015.07.004

Bourrat, X., Francke, L., Lopez, E., Rousseau, M., Stempfle, P., Angellier, M., Alberic, P., 2007. Nacre biocrystal thermal behaviour. R. Soc. Chem. 9, 1205-1208. doi:10.1039/b709388h

Broadhurst, C.L., Wang, Y., Crawford, M.A., Cunnane, S.C., Parkington, J.E., Schmidt, W.F., 2002. Brain-specific lipids from marine, lacustrine, or terrestrial food resources: Potential impact on early African *Homo sapiens*. Comp. Biochem. Physiol. - B Biochem. Mol. Biol. 131, 653-673. doi:10.1016/S1096-4959(02)00002-7

Burchell, M., Cannon, A., Hallmann, N., Schwarcz, H.P., Schöne, B.R., 2013. Refining estimates for the season of shellfish collection on the Pacific Northwest coast: Applying high-resolution stable oxygen isotope analysis and sclerochronology. Archaeometry 55, 258-276. doi:10.1111/j.1475-4754.2012.00684.x

Butler, P.G., Wanamaker, A.D., Scourse, J.D., Richardson, C.A., Reynolds, D.J., 2013. Variability of marine climate on the North Icelandic Shelf in a 1357-year proxy archive based on growth increments in the bivalve *Arctica Islandica*. Palaeogeogr. Palaeoclimatol. Palaeoecol. 373, 141-151. doi:10.1016/j.palaeo.2012.01.016

Carlen, A., Olafsson, E., 2002. The effects of the gastropod *Terebralia palustris* on infaunal communities in a tropical tidal mud-flat in East Africa. Wetl. Ecol. Manag. 10, 303-311.

Carter, R., 1997. The Wadi Suq period in south-east Arabia: a reappraisal in the light of excavations at Kalba, UAE. Proc. Semin. Arab. Stud. 27, 87-98.

Carter, J.G., Harries, P.J., Malchus, N., Sartori, A.F., Anderson, L.C., Bieler, R., Bogan, A.E., Coan, E.V., Cope, J.C.W., Cragg, S.M., Garcia-March, J.R., Hylleberg, J., Kelley, P., Kleemann, K., Kriz, J., McRoberts, C., Mikkelsen, P.M., Pojeta, J.J., Temkin, I., Yancey, T., Zieritz, A., 2012. Illustrated glossary of the bivalvia. Treatise Online 1, 209.

Colonese, A.C., Troelstra, S., Ziveri, P., Martini, F., Lo Vetro, D., Tommasini, S., 2009. Mesolithic shellfish exploitation in SW Italy: seasonal evidence from the oxygen isotopic composition of *Osilinus turbinatus* shells. J. Archaeol. Sci. 36, 1935-1944. doi:10.1016/j.jas.2009.04.021

Colonese, A.C., Mannino, M.A., Bar-Yosef Mayer, D.E., Fa, D.A., Finlayson, J.C., Lubell, D., Stiner, M.C., 2011. Marine mollusc exploitation in Mediterranean prehistory: An overview. Quat. Int. 239, 86-103. doi:10.1016/j.quaint.2010.09.001

Craig, O.E., Steele, V.L., Fischer, A., Hartz, S., Andersen, S.H., Donohoe, P., Glykou, A., Saul, H., Jones, M.D., Koch, E., Heron, C.P., 2011. Ancient lipids reveal continuity in culinary practices across the transition to agriculture in Northern Europe. Proc. Natl. Acad. Sci. U. S. A. 108, 17910-17915. doi:10.1073/pnas.0913714

Da Costa, M.A., 2015. Distribution and Shape Analysis of *Phorcus lineatus* and *Phorcus sauciatus* along the Portuguese Coast, Universidade de Lisboa.

de Lumley, H., 1966. Les fouilles de Terra Amata à Nice. Premiers résultats. Bulletin du Musée d'Anthropologie et Préhistoire de Monaco 13, 29-51.

Debono Spiteri C., Craig, O.E., 2014. Biomolecular and isotopic characterisation of lipid residues absorbed in Impressed Wares from the Early Neolithic village of Skorba, Malta. Malta Archaeol. Rev. 14-22.

Donald, K.M., Preston, J., Williams, S.T., Reid, D.G., Winter, D., Alvarez, R., Buge, B., Hawkins, S.J., Templado, J., Spencer, H.G., 2012. Phylogenetic relationships elucidate colonization patterns in the intertidal grazers *Osilinus* Philippi, 1847 and *Phorcus* Risso, 1826 (Gastropoda: Trochidae) in the northeastern Atlantic Ocean and Mediterranean Sea. Mol. Phylogenet. Evol. 62, 35-45. doi:10.1016/j.ympev.2011.09.002

Douka, K., Jacobs, Z., Lane, C., Grün, R., Farr, L., Hunt, C., Inglis, R.H., Reynolds, T., Albert, P., Aubert, M., Cullen, V., Hill, E., Kinsley, L., Roberts, R.G., Tomlinson, E.L., Wulf, S., Barker, G., 2014. The chronostratigraphy of the Haua Fteah cave (Cyrenaica, northeast Libya). J. Hum. Evol. 66, 39-63. doi:10.1016/j.jhevol.2013.10.001

Eerkens, J.W., Byrd, B.F., Spero, H.J., Fritschi, A.K., 2013. Stable isotope reconstructions of shellfish harvesting seasonality in an estuarine environment: Implications for Late Holocene San Francisco Bay settlement patterns. J. Archaeol. Sci. 40, 2014-2024. doi:10.1016/j.jas.2012.12.018

Erlandson, J.M., 2001. The archaeology of aquatic adaptations: paradigm for a new millennium. J. Archaeol. Res. 9, 287-350.

Erlandson, J.M., Rick, T.C., Vellanoweth, R.L., Kennett, D.J., 1999. Maritime subsistence at a 9300 year old shell midden on Santa Rosa Island, California. J. F. Archaeol. 26, 255-265. doi:10.1179/jfa.1999.26.3.255

Fa, D.A., 2008. Effects of tidal amplitude on intertidal resource availability and dispersal pressure in prehistoric human coastal populations: the Mediterranean-Atlantic transition. Quat. Sci. Rev. 27, 2194-2209. doi:10.1016/j.quascirev.2008.07.015

Farr, L. Lane, R., Abdulazeez, F., Bennett, P., Holman, J., Marasi, A., Prendergast, A., Al- Zweyi, M., Barker, G., 2014. The Cyrenaican Prehistory Project 2013: the seventh season of excavations in the Haua Fteah cave. Libyan Stud. 45, 163-173.

Ferguson, J.E., Henderson, G.M., Fa, D.A., Finlayson, J.C., Charnley, N.R., 2011. Increased seasonality in the Western Mediterranean during the last glacial from limpet shell geochemistry. Earth Planet. Sci. Lett. 308, 325-333. doi:10.1016/j.epsl.2011.05.054

Ford, P.J., 1989. Molluscan assemblages from archaeological deposits. Geoarchaeology 4, 157-173. doi:10.1002/gea.3340040205

Gardner, A.S., 2005. Marine mollusc shells from two archaeological sites near Al Ain. Tribulus 15.1, 9-12.

Girod, A. 2011. Land snails from Late Glacial and Early Holocene Italian sites. Quaternary International 244, 105-116.

Gomez-Villalba, L.S., Lopez-Arce, P., Alvarez de Buergo, M., Fort, R., 2012. Atomic defects and their relationship to aragonite-calcite transformation in portlandite nanocrystal carbonation. Cryst. Growth Des. 12, 4844-4852.

Goodwin, D.H., Flessa, K.W., Schöne, B.R., Dettman, D.L., 2001. Cross-calibration of daily growth increments, stable isotope variation, and temperature in the Gulf of California bivalve mollusk *Chione cortezi*: Implications for palaeoenvironmental analysis. Palaios 16, 387-398. doi:10.1669/0883-1351(2001)016

Greengo, R.E., 1952. Shellfish of the California Indians. Kroeber Anthropol. Soc. 7, 63-114.

Gutiérrez-Zugasti, I., Garcia-Escarzaga, A., Martin-Chivelet, J., Gonzalez-Morales, M.R., 2015. Determination of sea surface temperatures using oxygen isotope ratios from *Phorcus lineatus* (Da Costa, 1778) in northern Spain: Implications for paleoclimate and archaeological studies. The Holocene 25, 1002-1014. doi:10.1177/0959683615574892

Hammond, H. 2014. Taphonomic analysis of archaeomalacological assemblages: shell middens on the northern coast of Santa Cruz (Patagonia, Argentina). Intersecciones in Antropologia Suppl. 15 (1).

Händel, M., 2013. Al-Hamriya - Dynamik einer Muschelhaufenlandschaft in den Vereinigten Arabischen Emiraten. Archaeologia Austriaca, 77-96.

Herbert, J.M., 2008. The history and practice of shell tempering in the Middle Atlantic: A useful balance. Southeast. Archaeol. 27, 265-285.

Hill E.A., Reimer, P.J., Hunt, C.O., Prendergast, A.L., Barker, G.W., 2017. Radiocarbon ecology of the land snail *Helix melanostoma* in Northeast Libya. Radiocarbon 59, 1-22. doi: 10.1017/RDC.2017.49

Houbrick, R.S., 1991. Systematic review and functional morphology of the mangrove snails *Terebralia* and *Telescopium* (Potamididae; Prosobranchia). Malacologia 33, 289-338

Huang, Z., Li, X., 2009. Nanoscale structural and mechanical characterization of heat treated nacre. Mater. Sci. Eng. C 29, 1803-1807. doi:10.1016/j.msec.2009.02.007

Hunt, C.O., Reynolds, T.G., El-Rishi, H., Buzaian, A., Hill, E., Barker, G.W., 2011. Resource pressure and environmental change on the North African littoral: Epipalaeolithic to Roman gastropods from Cyrenaica, Libya. Quat. Int. 244, 15-26. doi:10.1016/j.quaint.2011.04.045

James, S.R., Dennell, R.W., Gilbert, A.S., Lewis, H.T., Gowlett, J.A.J., Lynch, T.F., Mcgrew, W.C., Peters, C.R., Pope, G.G., Stahl, A.B., 1989. Hominid use of fire in the Lower and Middle Pleistocene: A review of the evidence. Curr. Anthropol. 30, 1-26. doi:10.2307/2743299

Jones, D.S., 1983. Sclerochronology: Reading the record of the molluscan shell. Am. Sci. 71, 384-391.

Kendall, M.A., 1987. The age and structure of some northern populations of the trochid gastropod *Monodonta lineata*. J. Molluscan Stud. 53, 213-222.

Kingery, W.D., Bowen, H.K., Uhlmann, D.R.,1976. Introduction to Ceramics. John Willey and Sons, New York.

Kobayashi, I., Samata, T., 2006. Bivalve shell structure and organic matrix. Mater. Sci. Eng. C 26, 692-698. doi:10.1016/j.msec.2005.09.101

Koga, N., Kasahara, D., Kimura, T., 2013. Aragonite crystal growth and solid-state aragonite-calcite transformation: A physico-geometrical relationship via thermal dehydration of included water. Cryst. Growth Des. 13, 2238-2246. doi:10.1021/cg400350w

Kroeber, A.L., Barrett, S.A., 1960. Fishing among the indians of Northwestern California, University of California Anthropological Records.

Kromer, B., Lindauer, S., Synal, H., Wacker, L., 2013. A new AMS facility at the Curt-Engelhorn-Centre for Achaeometry, Mannheim, Germany. Nucl. Inst. Methods Phys. Res. B 294, 11-13. doi:10.1016/j.nimb.2012.01.015

Lanting, J.N., Aerts-Bijma, A.T., van der Plicht, J., 2001. Dating of cremated bones. Radiocarbon 43, 249-254. doi:10.2458/azu_js_rc.v.3946

Lécuyer, C., 1996. Effects of heating on the geochemistry of biogenic carbonates. Chem. Geol. 129, 173-183. doi:10.1016/0009-2541(96)00005-8

Lindauer, S., Marali, S., Schöne, B.R., Uerpmann, H.-P., Kromer, B., Hinderer, M., 2016. Investigating the local reservoir age and stable isotopes of shells from Southeast Arabia. Radiocarbon 1-18. doi:10.1017/RDC.2016.80

Lindauer, S., Santos, G.M., Steinhof, A., Yousif, E., Phillips, C., Jasim, S.A., Uerpmann, H.P., Hinderer, M., 2017. The local marine reservoir effect at Kalba (UAE) between the Neolithic and Bronze Age:

An indicator of sea level and climate changes. Quat. Geochronol. 42, 105–116. https://doi.org/10.1016/j.quageo.2017.09.003

Liu, M.L., Yund, R.A., 1993. Transformation kinetic of polycristalline aragonite to calcite: new experimental data, modelling and implications. Contrib. to Mineral. Petrol. 114, 465-478. doi:10.1007/BF00321751

Maggetti, M., Neururer, C., Ramseyer, D., 2011. Temperature evolution inside a pot during experimental surface (bonfire) firing. Appl. Clay Sci. 53, 500-508. doi:10.1016/j.clay.2010.09.013

Mannino, M.A., Thomas, K.D., 2001. Intensive Mesolithic exploitation of coastal resources? Evidence from a shell deposit on the Isle of Portland (Southern England) for the impact of human foraging on populations of intertidal rocky shore molluscs. J. Archaeol. Sci. 1101-1114. doi:10.1006/jasc.2001.0658

Mannino, M.A., Thomas, K.D., 2002. Depletion of a resource? The impact of prehistoric human foraging on intertidal mollusc communities and its significance for human settlement, mobility and dispersal. World Archaeol. 33, 452-474. doi:10.1080/00438240120107477

Mannino, M.A., Spiro, B.F., Thomas, K.D., 2003. Sampling shells for seasonality: oxygen isotope analysis on shell carbonates of the inter-tidal gastropod *Monodonta lineata* (da Costa) from populations across its modern range and from a Mesolithic site in southern Britain. J. Archaeol. Sci. 30, 667-679. doi:10.1016/S0305-4403(02)00238-8

Mannino, M.A., Thomas, K.D., Leng, M.J., Piperno, M., Tusa, S., Tagliacozzo, A., 2007. Marine resources in the mesolithic and neolithic at the Grotta dell'Uzzo (Sicily): Evidence from isotope analyses of marine shells. Archaeometry 49, 117-133. doi:10.1111/j.1475-4754.2007.00291.x

Mannino, M.A., Thomas, K.D., Leng, M.J., Sloane, H.J., 2008. Shell growth and oxygen isotopes in the topshell *Osilinus turbinatus*: resolving past inshore sea surface temperatures. Geo-Marine Lett. 28, 309-325. doi:10.1007/s00367-008-0107-5

Marean, C.W., Bar-Matthews, M., Bernatchez, J.A., Fisher, E.C., Goldberg, P., Herries, A.I.R., Jacobs, Z., Jerardino, A., Karkanas, P., Minichillo, T., Nilssen, P.J., Thompson, E., Watts, I., Williams, H.M., 2007. Early human use of marine resources and pigment in South Africa during the Middle Pleistocene. Nature 449, 906-909. doi:10.1038/nature06204

Maritan, L., Mazzoli, C., Freestone, I., 2007. Modelling changes in mollusc shell internal microstructure during firing: Implications for temperature estimation in shell-bearing pottery. Archaeometry 49, 529-541. doi:10.1111/j.1475-4754.2007.00318.x

McBurney, C.B.M. (Ed.), 1967. The Haua Fteah (Cyrenaica) and the Stone Age of the South-East Mediterranean. Cambridge University Press, Cambridge.

Meehan, B., 1977. Hunters by the seashore. J. Hum. Evol. 6, 363-370.

Meehan, B., 1982. Shell Bed to Shell Midden. Australian Institute of Aboriginal Studies, Canberra.

Menzies, R., Cohen, Y., Lavie, B., Nevo, E., 1992. Niche adaptation in two marine gastropods, *Monodonta turbiformis* and *M. turbinata*. Bolletino di Zool. 59, 297-302. doi:10.1080/11250009209386685

Milano, S., Prendergast, A.L., Schöne, B.R., 2016. Effects of cooking on mollusk shell structure and chemistry: Implications for archeology and palaeoenvironmental reconstruction. J. Archaeol. Sci. Reports 7, 14-26. doi:10.1016/j.jasrep.2016.03.045

Milano, S., Schöne, B.R., Witbaard, R., 2017. Changes of shell microstructural characteristics of *Cerastoderma edule* (Bivalvia) - A novel proxy for water temperature. Palaeogeogr. Palaeoclimatol. Palaeoecol. 465, 395-406. doi:10.1016/j.palaeo.2015.09.051

Miyaji, T., Tanabe, K., Schöne, B.R., 2007. Environmental controls on daily shell growth of *Phacosoma japonicum* (Bivalvia: Veneridae) from Japan. Mar. Ecol. Prog. Ser. 336, 141-150. doi:10.3354/meps336141

Mook, W., 1971. Paleotemperatures and chlorinities [CORRECT?] from stable carbon and oxygen isotopes in shell carbonate. Palaeogeogr. Palaeoclimatol. Palaeoecol. 9, 245-263. doi:10.1016/0031-0182(71)90002-2

Moss, M.L., 1993. Shellfish, gender, and status on the Northwest coast: reconciling archeological, ethnographic, and ethnohistorical records of the Tlingit. Am. Anthropol. 95, 631-652. doi:10.1525/aa.1993.95.3.02a00050

Mougne, C., Dupont, C., Giazzon, D., Quesnel, L., 2014. Shellfish from the Bronze Age Site of Clos des Châtaigniers (Mathieu, Normandy, France). Internet Archaeol. https://doi.org/10.11141/ia.37.5

Newton, R., Moss, M., 1984. The Subsistence Lifeway of the Tlingit People: Excerpts of Oral Interviews. USDA Forest Service Alaska Region Report No.179, Juneau.

Nishihira, M., Kuniyoshi, M., Shimamura, K., 2002. Size variation in *Terebralia palustris* (Gastropoda: Potamididae) of Iriomote Isl

and, southern Japan, and its effect on some population characteristics. Wetl. Ecol. Manag. 10, 243-247.

Oschmann, W., 2009. Sclerochronology: Editorial. Int. J. Earth Sci 98, 1-2. doi:10.1007/s00531-008-0403-3

Percy, G., 1608. Observations Gathered out of a Discourse of the Plantation of the Southern Colony in Virginia by the English, 1606.

Perdikouri, C., Kasioptas, A., Geisler, T., Schmidt, B.C., Putnis, A., 2011. Experimental study of the aragonite to calcite transition in aqueous solution. Geochim. Cosmochim. Acta 75, 6211-6224. doi:10.1016/j.gca.2011.07.045

Perić, J., Vučak, M., Krstulović, R., Brečević, L., Kralj, D., 1996. Phase transformation of calcium carbonate polymorphs. Thermochim. Acta 277, 175-186. doi:10.1016/0040-6031(95)02748-3

Petchey, F., Ulm, S., David, B., Mcniven, I.J., Asmussen, B., Tomkins, H., Dolby, N., Aplin, K., Richards, T., Rowe, C., Leavesley, M., 2013. High-resolution radiocarbon dating of marine materials in archaeological contexts : radiocarbon marine reservoir variability between *Anadara, Gafrarium, Batissa, Polymesoda* spp. and Echinoidea at Caution Bay, Southern Coastal Papua New Guinea. Archaeol. Anthropol. Sci. 5, 69-80. doi:10.1007/s12520-012-0108-1

Phillips, C.S., Mosseri-Marlio, C.E., 2002. Sustaining change: The emerging picture of the Neolithic to Iron Age subsistence economy at Kalba, Sharjah Emirate, UAE, in: Proceedings of the Fifth

International Symposium on the Archaeozoology of Southwestern Asia and Adjacent Areas. ARC-Publicaties, Groningen, The Netherlands. EDITOR(S)?

Plaziat, J.C., 1984. Mollusk distribution in the mangal. In: Por D, Dor I (eds) Hydrobiology of the mangal: the ecosystem of the mangrove forests. Junk, Boston, pp. 111-143.

Prendergast, A.L., Azzopardi, M., O'Connell, T.C., Hunt, C., Barker, G., Stevens, R.E., 2013. Oxygen isotopes from *Phorcus* (*Osilinus*) *turbinatus* shells as a proxy for sea surface temperature in the central Mediterranean: A case study from Malta. Chem. Geol. 345, 77-86. doi:10.1016/j.chemgeo.2013.02.026

Prendergast, A.L., Stevens, R.E., O'Connell, T.C., Fadlalak, A., Touati, M., Al-Mzeine, A., Schöne, B.R., Hunt, C.O., Barker, G.W., 2016. Changing patterns of eastern Mediterranean shellfish exploitation in the Late Glacial and Early Holocene : Oxygen isotope evidence from gastropods in Epipaleolithic to Neolithic human occupation layers at the Haua Fteah cave, Libya. Quat. Int. 407, 80-93. doi:10.1016/j.quaint.2015.09.035

Prendergast, A.L., Schöne, B.R., 2017. Oxygen isotopes from limpet shells: Implications for palaeothermometry and seasonal shellfish foraging studies in the Mediterranean. Palaeogeogr. Palaeoclimatol. Palaeoecol. 484, 33-47. doi:10.1016/j.palaeo.2017.03.007

Ragir, S., 2000. Diet and food preparation: Rethinking early hominid behavior. Evol. Anthropol. 9, 153-155. doi:10.1002/1520-6505(2000)9:4<153::AID-EVAN4>3.0.CO;2-D

Reagan, A.B., 1934. Various uses of plants by West Coast Indians. Washingt. Hist. Q. 25, 133-137.

Reimer, P.J., McCormac, F.G., 2002. Marine radiocarbon reservoir corrections for the Mediterranean and Aegean Seas. Radiocarbon 44, 159-166.

Reimer, P.J., Bard, E., Bayliss, A., Beck, J.W., Blackwell, P.G., Bronk, C., Caitlin, R., Hai, E.B., Edwards, R.L., 2013. Intcal13 and marine13 radiocarbon age calibration curves 0 - 50,000 years cal CP. Radiocarbon 55, 1869-1887. doi:http://doi.org/10.2458/azu_js_rc.55.16947

Rick, T.C., Lowery, D.L., 2013. Accelerator mass spectrometry 14C dating and the antiquity of shell-tempered ceramics from the Chesapeake Bay and Middle Atlantic. Am. Antiq. 78, 570-579.

Schembri, P.J., Deidun, A., Mallia, A., Mercieca, L., 2005. Rocky shore biotic assemblages of the Maltese Islands (Central Mediterranean): A conservation perspective. J. Coast. Res. 21, 157-166.

Schöne, B.R., 2008. The curse of physiology—challenges and opportunities in the interpretation of geochemical data from mollusk shells. Geo-Marine Lett. 28, 269-285. doi:10.1007/s00367-008-0114-6

Schöne, B.R., Freyre Castro, A.D., Fiebig, J., Houk, S.D., Oschmann, W., Kröncke, I., 2004. Sea surface water temperatures over the period 1884-1983 reconstructed from oxygen isotope ratios of a bivalve mollusk shell (*Arctica islandica*, southern North Sea). Palaeogeogr. Palaeoclimatol. Palaeoecol. 212, 215-232. doi:10.1016/j.palaeo.2004.05.024

Schöne, B.R., Fiebig, J., Pfeiffer, M., Gleß, R., Hickson, J., Johnson, A.L.A., Dreyer, W., Oschmann, W., 2005. Climate records from a bivalved Methuselah (*Arctica islandica*, Mollusca; Iceland). Palaeogeogr. Palaeoclimatol. Palaeoecol. 228, 130-148. doi:10.1016/j.palaeo.2005.03.049

Schöne, B.R., Krause, R.A., 2016. Retrospective environmental biomonitoring - Mussel Watch expanded. Glob. Planet. Change 144, 228-251. doi:10.1016/j.gloplacha.2016.08.002

Shackleton, N.J., 1973. Oxygen isotope analysis as a means of determining season of occupation of prehistoric midden sites. Archaeometry 15, 133-141. doi:10.1111/j.1475-4754.1973.tb00082.x

Smith, D., 1978. Delia Smith's Complete Cookery Course. BBC Publications, London.

Steinhardt, J., Butler, P.G., Carroll, M.L., Hartley, J., 2016. The application of long-lived bivalve sclerochronology in environmental baseline monitoring. Front. Mar. Sci. 3. doi:10.3389/fmars.2016.00176

Taché, K., Craig, O.E., 2015. Cooperative harvesting of aquatic resources and the beginning of pottery production in north-eastern North America. Antiquity 89, 177-190. doi:10.15184/aqy.2014.36

Taylor, V.K., Barton, R.N.E., Bell, M., Bouzouggar, A., Collcutt, S., Black, S., Hogue, J.T., 2011. The Epipalaeolithic (Iberomaurusian) at Grotte des Pigeons (Taforalt), Morocco: A preliminary study of the land Mollusca. Quat. Int. 244, 5-14. doi:10.1016/j.quaint.2011.04.041

Tebano, T., Paulay, G., 2001. Variable recruitment and changing environments create a fluctuating resource: The biology of *Anadara uropigimelana* (Bivalvia: Arcidae) on Tarawa atoll. Atoll Res. Bull. 488.

Thoms, A. V., 2008. The fire stones carry: Ethnographic records and archaeological expectations for hot-rock cookery in western North America. J. Anthropol. Archaeol. 27, 443-460. doi:10.1016/j.jaa.2008.07.002

Van Strydonck M., Boudon M., Hoefkens M., D.M.G., 2005. ^{14}C-dating of cremated bones, why does it work? Lunula. Archaeol. Protohistorica 13, 3-10.

Villagran, X.S., Balbo, A.L., Madella, M., Vila, A., Estevez, J., 2011. Experimental micromorphology in Tierra del Fuego (Argentina): building a reference collection for the study of shell middens in cold climates. J. Archaeol. Sci. 38, 588-604. doi:10.1016/j.jas.2010.10.013

Wacker, L., Fülöp, R., Hajdas, I., Molnár, M., Rethemeyer, J., 2013. A novel approach to process carbonate samples for radiocarbon measurements with helium carrier gas. Nucl. Inst. Methods Phys. Res. B 294, 214-217. doi:10.1016/j.nimb.2012.08.030

Waselkov, G.A., 1987. Shell gathering and shell midden archaeology. Adv. Archaeol. Method Theory 10, 93-209.

Wolf, M., Lehndorff, E., Wiesenberg, G.L.B., Stockhausen, M., Schwark, L., Amelung, W., 2013. Towards reconstruction of past fire regimes from geochemical analysis of charcoal. Org. Geochem. 55, 11-21. doi:10.1016/j.orggeochem.2012.11.002

Wrangham, R., 2009. Catching Fire: How Cooking Made Us Human. Basic Books, New York.

Yoshioka, S., Kitano, Y., 1985. Transformation of aragonite to calcite through heating. Geochem. J. 19, 245-249.

Zolotoyabko, E., Pokroy, B., 2007. Biomineralization of calcium carbonate: structural aspects. CrystEngComm 9, 1156-1161. doi:10.1039/b710974a

Figure and tables

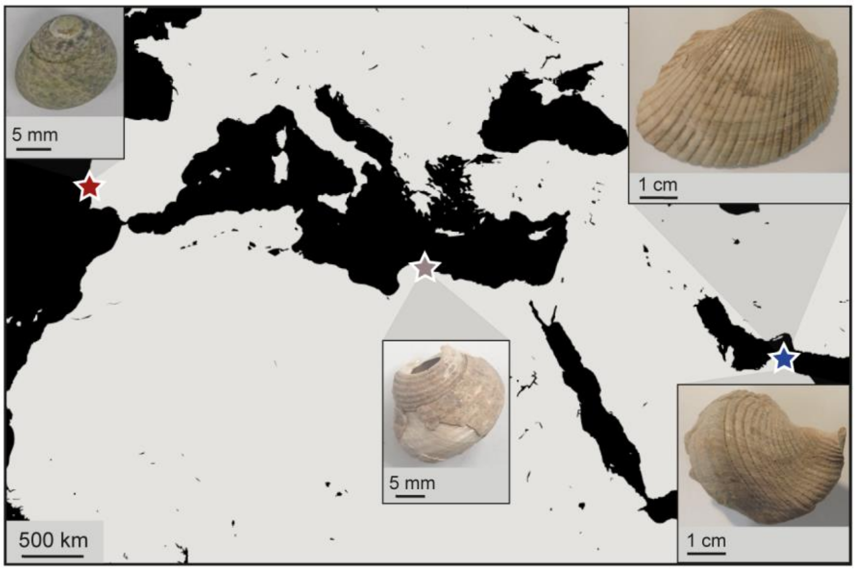

Fig. 1. Map showing the localities encompassed in the study. Red star: Praia do Tamariz, Portugal, where the modern *Phorcus lineatus* were collected. Grey star: Haua Fteah cave, Libya, where the archaeological *Phorcus turbinatus* were excavated. Blue star: sites in the UEA from which the archaeological remains of *Anadara uropigimelana* and *Terebralia palustris* were excavated.

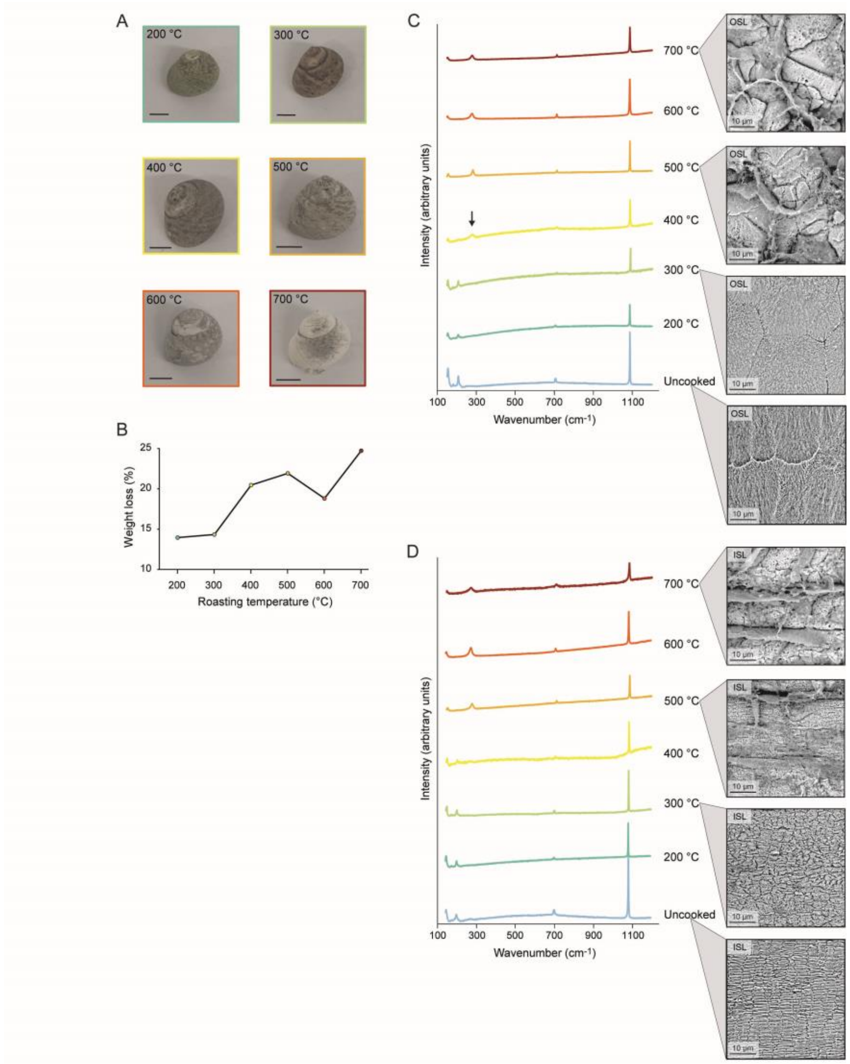

Fig. 2. Effects of the 5-minute heating experiment on *P. lineatus* shell. (A) Overall shell appearance after the thermal exposure at different temperatures. Scale bars = 5 mm. (B) Shell weight loss in response to heat. (C) Effect of heat on the outer shell layer (OSL) mineralogy and microstructures. The black arrow shows the extra peak in the 400 °C Raman spectrum indicating the transition phase from aragonite into calcite. (D) Thermal response of the inner shell layer (ISL) mineralogy and microstructures.

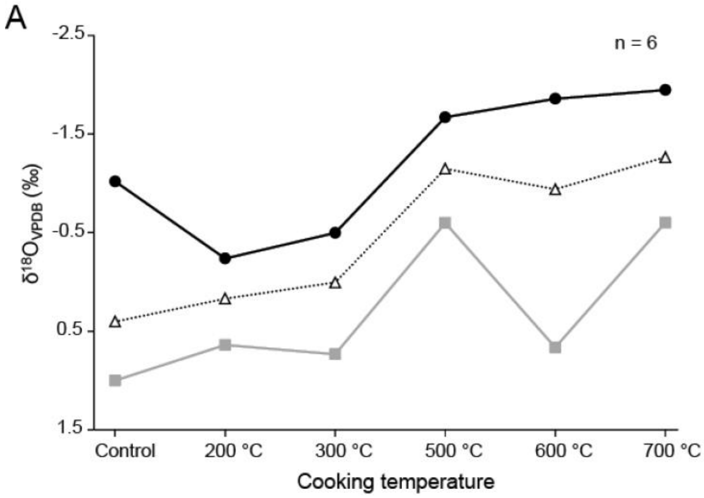

B

Cooking temperature	$\delta^{18}O_{shell}$ (p value)		
	5 min	20 min	60 min
100 °C	NA		
200 °C		NA	NA
300 °C			
500 °C			
600 °C		NA	NA
700 °C			

Fig. 3. Thermal behaviour of shell oxygen isotopes. (A) Oxygen isotope composition after roasting at the different temperatures. Gray squares=maximum $\delta^{18}O_{shell}$; open triangles=average $\delta^{18}O_{shell}$; black circles=minimum $\delta^{18}O_{shell}$. (B) The table refers to the different cooking durations tested in the present study and the previous study by Milano et al. (2016). Green cells indicate statistical similarity between isotope values of the heated and control shells ($p > 0.05$). Red cells indicate statistical difference ($p < 0.05$). The yellow cell relates to a disagreement in the case of the specimen roasted at 300 °C for 20 minutes. Its isotopic signature was statistically similar to the one of the control shell but different to the second control sample.

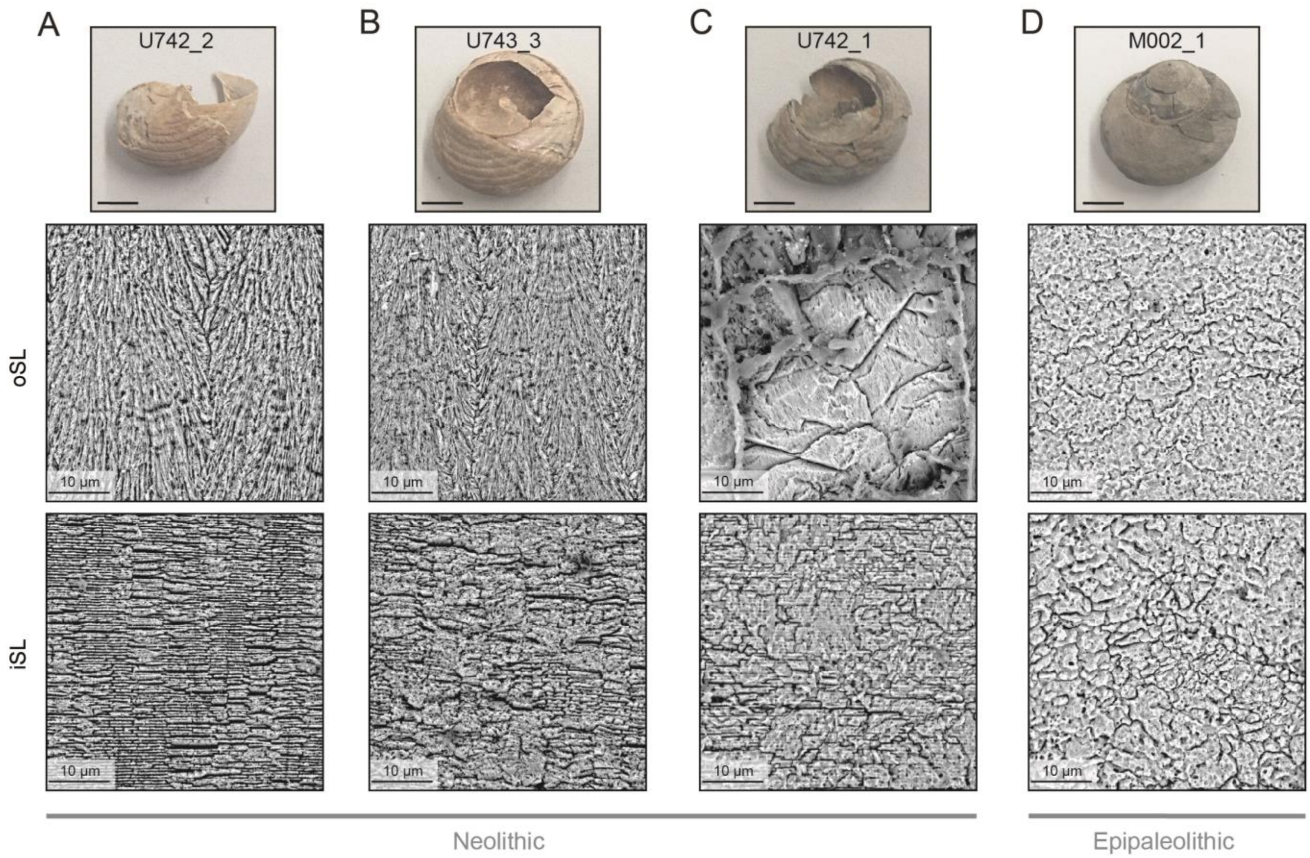

Fig. 4. Macroscopic appearance and microstructural organization of *P. turbinatus* shells from (A-C) Neolithic contexts and (D) Mesolithic contexts in the Haua Fteah cave. The first row of SEM images refers to the prismatic microstructures of the OSL. The second row displays the nacre platelets of the ISL. The visible changes in structural organization denote possible exposure to heating processes. Scale bars if not otherwise indicated = 5 mm.

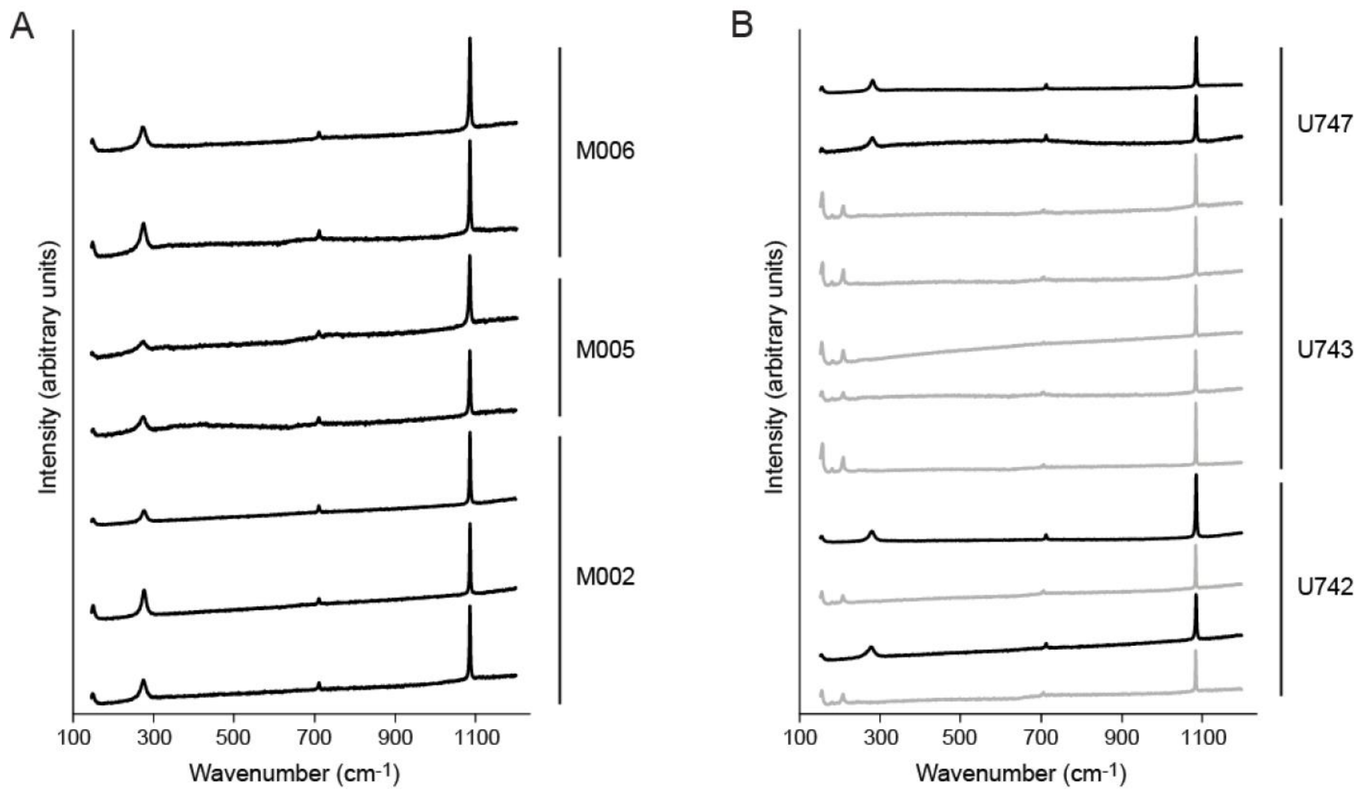

Fig. 5. Raman spectra of *P. turbinatus* ISLs from (A) Neolithic contexts and (B) Mesolithic contexts in the Haua Fteah cave. All Mesolithic specimens and four Neolithic specimens were calcitic (black lines); the rest of the Neolithic specimens were aragonitic (grey lines).

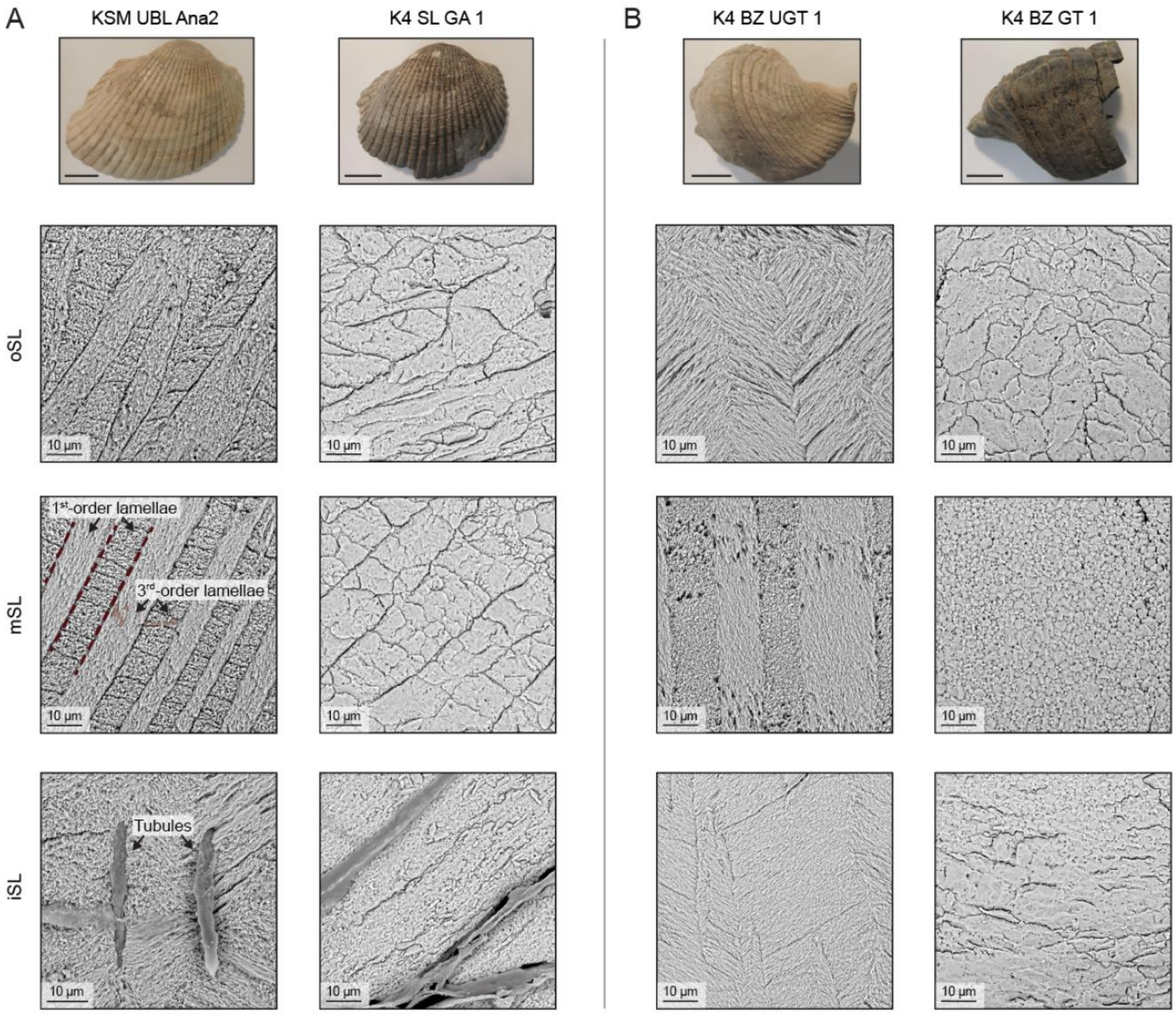

Fig. 6. Macroscopic appearance and microstructural organization of the archaeological shells from the United Arab Emirates. (A) Whole shell and SEM images of two *A. uropigimelana* specimens. Shell KSM UBL Ana2 showed the typical microstructural architecture of the species. Highlights on the SEM images indicate the first and third order units of the crossed-lamellar structures as well as the organic microtubules perforating the shell material. Specimen K4 SL GA 1 shows the alteration of the overall color and microstructures, possible related to heat treatment. (B) Whole shell and SEM images of two *T. palustris* specimens with regular (K4 BZ UGT 1) and altered microstructures and appearance (K4 BZ UGT 1). Scale bars if not otherwise indicated = 1 cm.

Fig. 7. Raman spectra of (A) *A. uropigimelana* and (B) *T. palustris* from the United Arab Emirates archaeological sites. Specimens K4 SL Ana2 and K4 BZ UGT 1 preserve their aragonitic OSL, MSL and ISL (grey lines). Specimens K4 SL GA 1 and K4 BZ GT 1 display calcite in all shell layers (black lines).

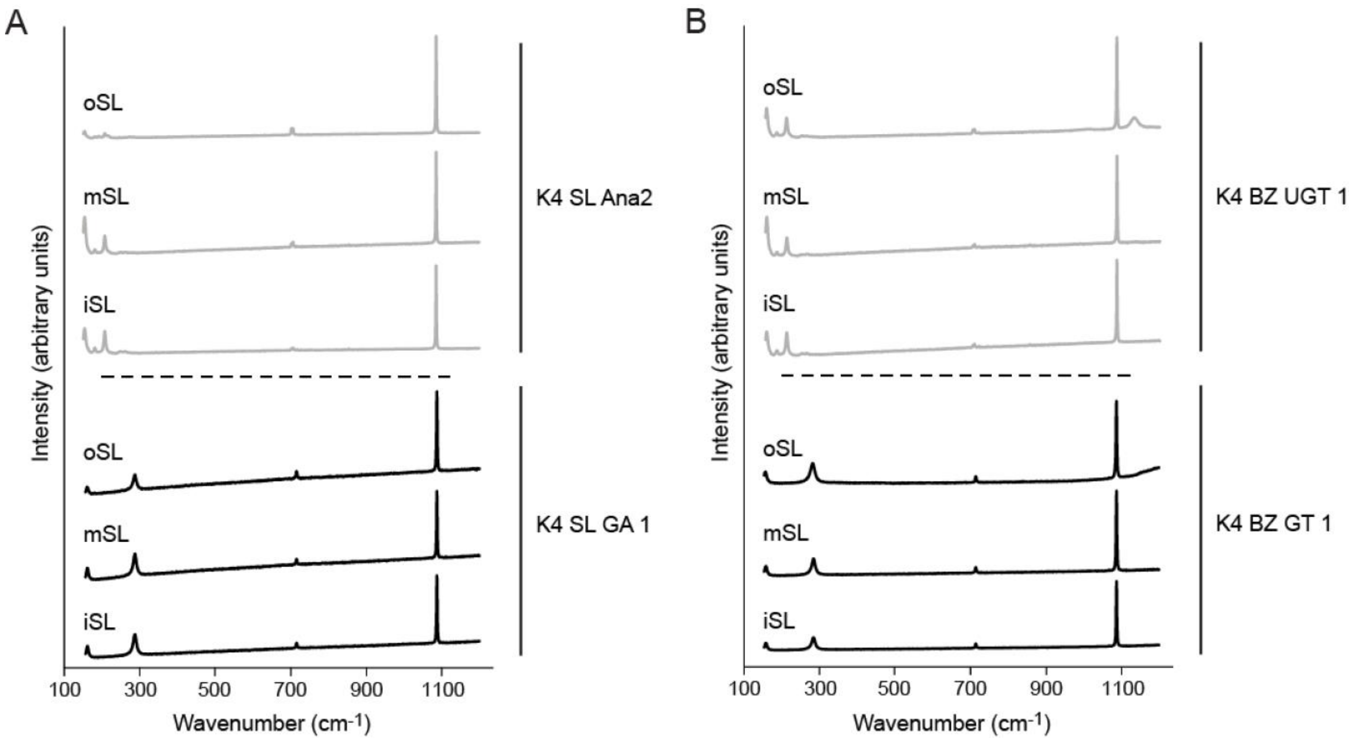

Fig. 8. Distribution of calibrated ^{14}C dates of Haua Fteah Trench U. Color-coding corresponds to the different materials used in the dating. Green = *H. Melanostoma* shells; blue = well-preserved *P. turbinatus*; grey = *P. turbinatus* from this study; black = charcoal.

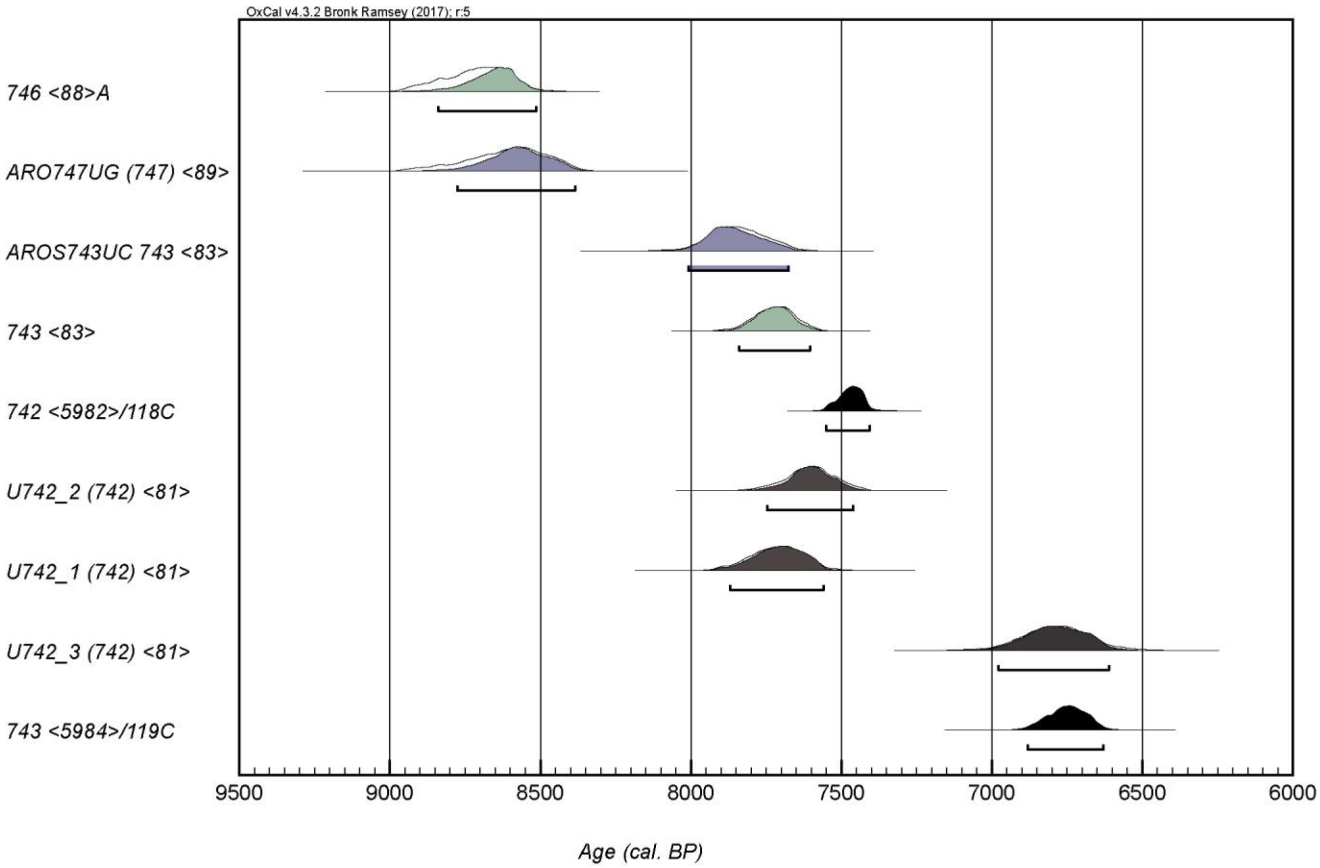

Table 1. List of studied specimens and details on their provenance.

ID	Species	Provenance	Period
A001	*P. lineatus*	Portugal	Modern
A001_M	*P. lineatus*	Portugal	Modern
A001_MR	*P. lineatus*	Portugal	Modern
A200	*P. lineatus*	Portugal	Modern
A200_M	*P. lineatus*	Portugal	Modern
A300	*P. lineatus*	Portugal	Modern
A300_M	*P. lineatus*	Portugal	Modern
A400	*P. lineatus*	Portugal	Modern
A400_M	*P. lineatus*	Portugal	Modern
A500	*P. lineatus*	Portugal	Modern
A500_M	*P. lineatus*	Portugal	Modern
A600	*P. lineatus*	Portugal	Modern
A600_M	*P. lineatus*	Portugal	Modern
A700	*P. lineatus*	Portugal	Modern
A700_M	*P. lineatus*	Portugal	Modern
M006_1	*P. turbinatus*	Haua Fteah, Libya	Capsian

M006_2	*P. turbinatus*	Haua Fteah, Libya	Capsian
M005_1	*P. turbinatus*	Haua Fteah, Libya	Capsian
M005_2	*P. turbinatus*	Haua Fteah, Libya	Capsian
M002_1	*P. turbinatus*	Haua Fteah, Libya	Capsian
M002_2	*P. turbinatus*	Haua Fteah, Libya	Capsian
M002_3	*P. turbinatus*	Haua Fteah, Libya	Capsian
U747_1	*P. turbinatus*	Haua Fteah, Libya	Neolithic
U747_2	*P. turbinatus*	Haua Fteah, Libya	Neolithic
U747_3	*P. turbinatus*	Haua Fteah, Libya	Neolithic
U743_1	*P. turbinatus*	Haua Fteah, Libya	Neolithic
U743_2	*P. turbinatus*	Haua Fteah, Libya	Neolithic
U743_3	*P. turbinatus*	Haua Fteah, Libya	Neolithic
U743_4	*P. turbinatus*	Haua Fteah, Libya	Neolithic
U742_1	*P. turbinatus*	Haua Fteah, Libya	Neolithic
U742_2	*P. turbinatus*	Haua Fteah, Libya	Neolithic
U742_3	*P. turbinatus*	Haua Fteah, Libya	Neolithic
U742_4	*P. turbinatus*	Haua Fteah, Libya	Neolithic
K4 SL Ana3	*A. uropigimelana*	Oman Sea	Bronze Age
K4 SL GA1	*A. uropigimelana*	Oman Sea	Bronze Age
K4 BZ GT1	*T. palustris*	Oman Sea	Bronze Age
K4 BZ UGT1	*T. palustris*	Oman Sea	Bronze Age
KSM UBL Ana2	*A. uropigimelana*	Oman Sea	Neolithic
KS Ana 1	*A. uropigimelana*	Oman Sea	Neolithic
KK1 Ana3	*A. uropigimelana*	Oman Sea	Neolithic

KK1 Ana4	*A. uropigimelana*	Oman Sea	Neolithic

Table 2. Reconstruction of shell exposure temperature by using shell overall appearance, microstructures and mineralogy as proxies in archeological specimens of *P. turbinatus*.

Shell ID	Reconstructed cooking temperature		
	Macroscale appearance	Microstructures	Mineralogy
M006_1	600 °C	600 °C	≥ 500 °C
M006_2	600 °C	600 °C	≥ 500 °C
M005_1	600 °C	600 °C	≥ 500 °C
M005_2	600 °C	600 °C	≥ 500 °C
M002_1	600 °C	700 °C	≥ 500 °C
M002_2	600 °C	600 °C	≥ 500 °C
M002_3	600 °C	700 °C	≥ 500 °C
U747_1	500 °C	600 °C	≥ 500 °C
U747_2	500 °C	600 °C	≥ 500 °C
U747_3	500 °C	300 °C	< 500 °C
U743_1	300 °C	300 °C	< 500 °C
U743_2	300 °C	300 °C	< 500 °C
U743_3	300 °C	300 °C	< 500 °C
U743_4	300 °C	300 °C	< 500 °C
U742_1	400 °C	500 °C	≥ 500 °C
U742_2	Not cooked	Not cooked	< 500 °C
U742_3	500 °C	600 °C	≥ 500 °C
U742_4	500 °C	300 °C	< 500 °C

Table 3. Trench U (Haua Fteah) ^{14}C dates. Symbol [*1] indicates dates corrected using reservoir offset of 58 ± 85 ^{14}C years (Reimer and McCormac, 2002). Symbol [*2] indicates dates corrected using reservoir offset of 476 ± 48 ^{14}C years (Hill et al., 2017).

Sample ID	**Lab Code**	**Material**	**Age (^{14}C yr)**	**±**	**Age (cal. BP) (unmodelled)**	**Age (cal. BP) (modelled)**
U742_1	MAMS 30538 U742-1	*P. Turbinatus*	7300	21	7901 - 7556[*1]	7869 - 7560[*1]
U742_2	MAMS 30538 U742-2	*P. Turbinatus*	7184	21	7772 - 7438[*1]	7747 - 7461[*1]
U742_3	MAMS 30538 U742-3	*P. Turbinatus*	6378	21	7002 - 6558[*1]	6978 - 6610[*1]
ARO747UG	OxA-27391	*P. Turbinatus*	8171	37	8891 - 8381[*1]	8776 - 8385[*1]
ARO747UC	OxA-27490	*P. Turbinatus*	7447	35	8024 - 7652[*1]	8008 - 7675[*1]
742 <5982>/118C	UBA-28873	Charcoal	6965	39	7551 - 7405	7551 - 7405
743<5984>/119C	UBA-28874	Charcoal	6291	50	6883 - 6627	6880 - 6630
746 <88> A	UBA-25915	*H. Melanostoma*	8670	39	8930 - 8534[*2]	8840 - 8531[*2]
743 <83>	UBA-25912	*H. Melanostoma*	7732	37	7850 - 7590[*2]	7840 - 7605[*2]

Supplementary material

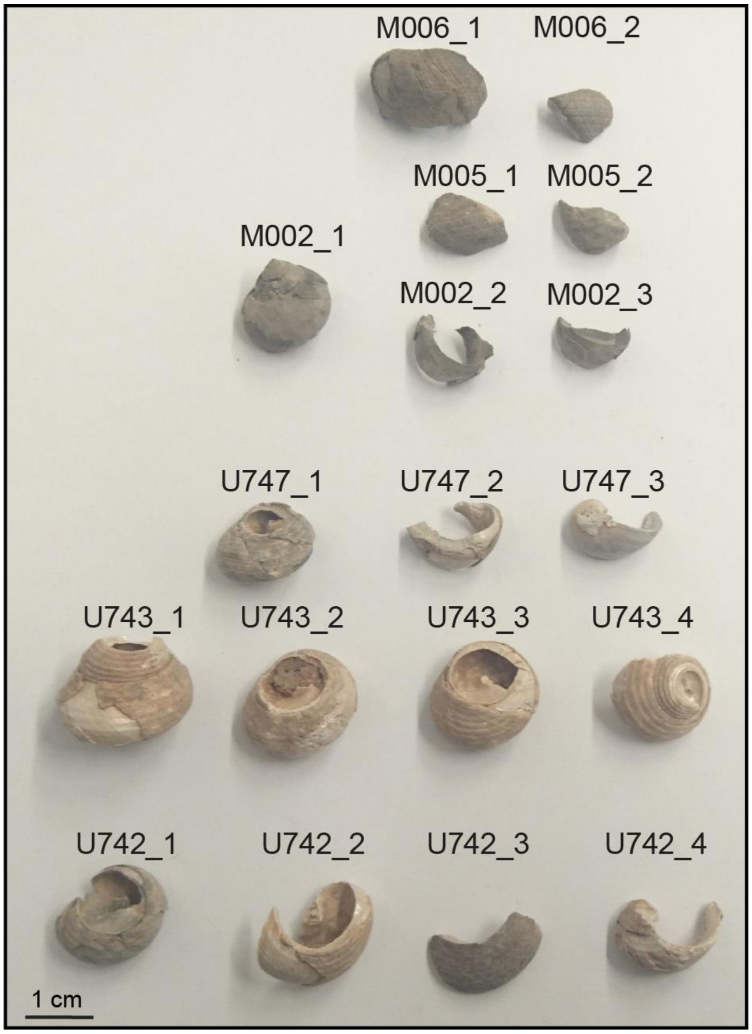

Fig. S1. Overall appearance of all *P. turbinatus* excavated from Haua Fteah cave and used in the present study. The upper seven specimens were excavated from Trench M (Mesolithic). The rest of the specimens were excavated from Trench U (Neolithic).

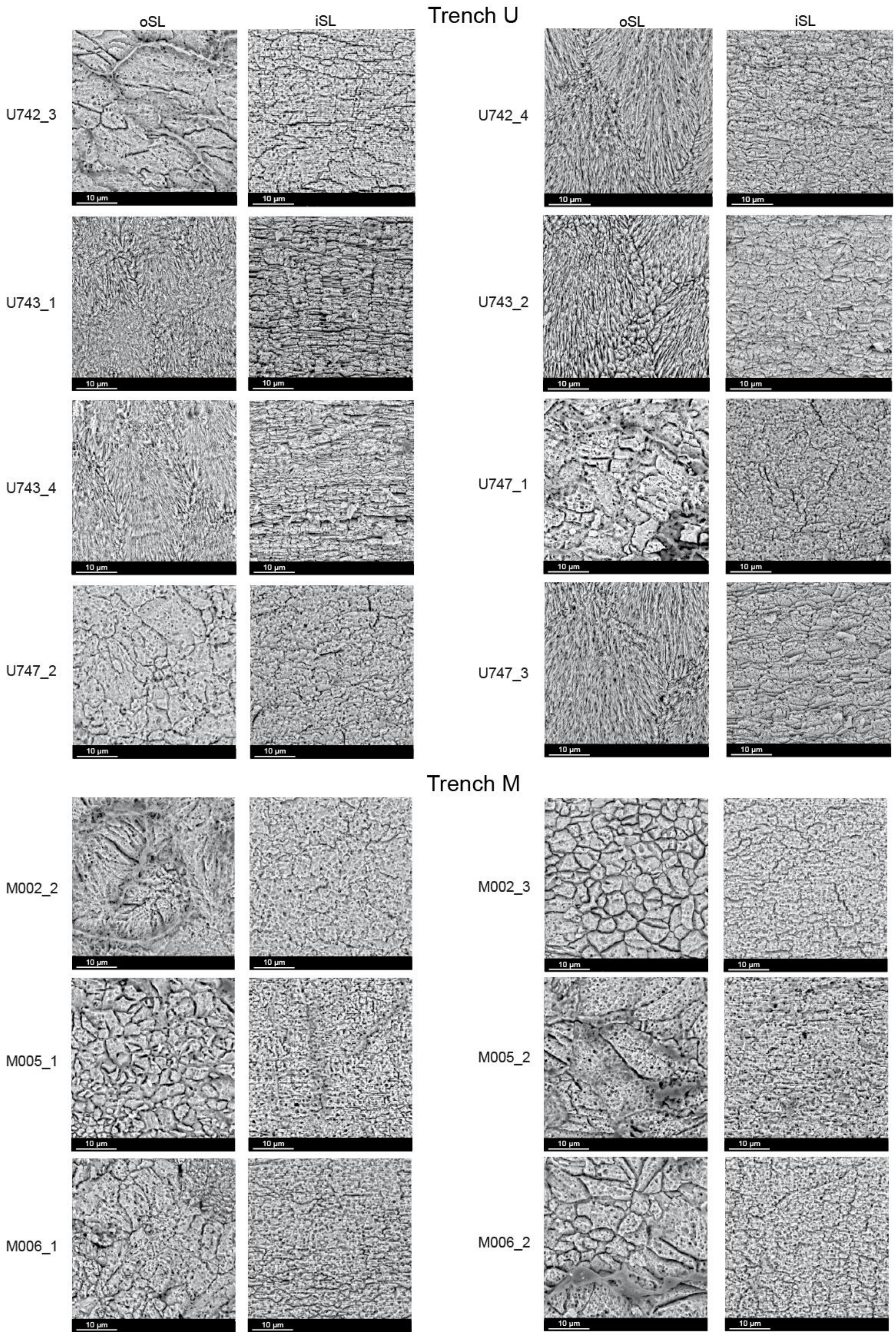
Trench U
oSL
iSL
oSL
iSL
U742_3
U742_4
U743_1
U743_2
U743_4
U747_1
U747_2
U747_3
Trench M
M002_2
M002_3
M005_1
M005_2
M006_1
M006_2
10 µm

Fig. S2.SEM images of the microstructural organization of *P. turbinatus* from Haua Fteah. Trench U = Neolithic context. Trench M = Mesolithic context.

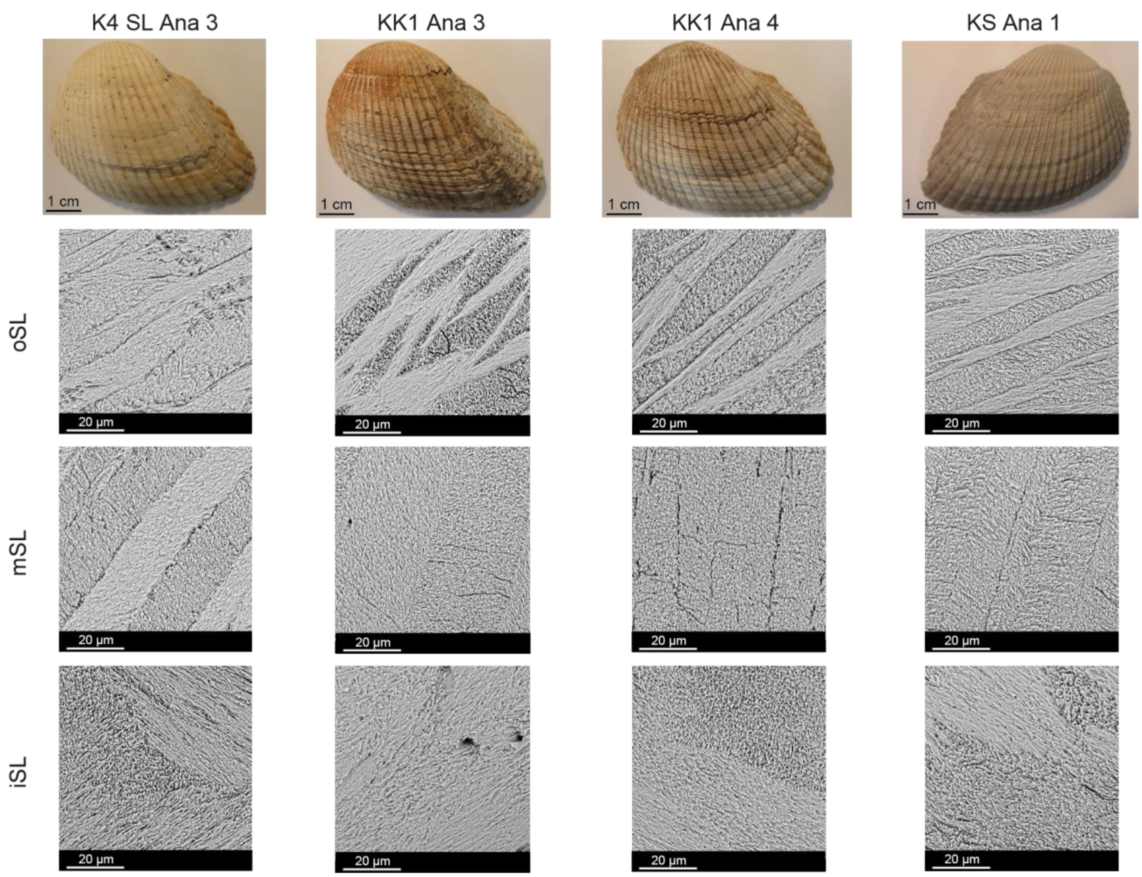

Fig. S3. Overall appearance and microstructural organization of *A. uropigimelana* from Southeast Arabia.